Title: Development and Control of converter for 1.5 MW PMSG

-Develop a suitable converter for the machine side including losses.

-Design the converter for the rated parameter of the machine.

submitted on 14.03.2019 –

by

Md.Nura Alam | Max Planck Straße Hausnr. 3 | PLZ: 18059 Ort: Rostock | e-Mail: md.alam@uni-rostock.de

Matriculation -Nr.: 217205705

Supervisor:
Name: Prof. Dr. rer. nat. habil. Uwe Ritschel
University of Rostock
Endowed Chair for Wind Energy Technology Stelzengang
Albert-Einstein-Str. 2
18059 Rostock

Second supervisor:
Name: Dipl.-Ing. Stefan Ganzel
University of Rostock
Endowed Chair for Wind Energy Technology Stelzengang
Albert-Einstein-Str. 2
18059 Rostock

Statutory Declaration

First Name	Md.Nura
Last Name	Alam
Matriculation Number	217205705
Master Course	Electrical Engineering
Date of Submission	02.03.2019

Hereby I declare on oath, that I, Md.Nura Alam, have authored in- dependently this report with the title Development and Control of Inverter for 1.5 MW PMSG and did not use any other means than indicated. The parts of the work which have been taken in the wording or meaning of other works are indicated in each case with naming of the original reference.

....

Place,Date Signature

Table of Contents

List of Figures

List of Tables

1. Introduction

The production of the wind power is increasing day by day in every parts of the world.Statistics show that for the last 5 years the wind power generation has increased 36% each year.The interconnection of the wind energy with the grid has made it more promising in the last few decades. [1] In order to connect the wind power with the grid require a sophisticated system interface. But the continous change of the wind is responsible of the various real,reactive output power and variable frequency of the power.For this reason it is essential to convert the generated ac power to a ac power of different frequency according to the grid requirement.

Additionaly,The conversion of an AC source to a different frequency AC source require different kind of high capacity electronic circuits like power converters,controllable power electronic devices.The intoduction of fast semiconductor switches which can handle high powers and computer as a real time controller have made it possible to connect the wind turbine with the grid efficiently. [2]

1.1 Wind Power System Topology

The PMSG based 1.5 MW wind turbine system topology is shown in Figure 1 below. The PMSG is directly connected with the wind turbine without a gear box since the number of pole pair in a PMSG is high . [3] In order to control the speed, torque and electrical braking system the generator is connected with the Speed and current controller via the generator side vector control system. The individual blocks of the figure will be explained below. Through the generator side converter the dc link capacitor is charged. The grid side converter takes power from the dc link capacitor and can control the reactive and active power which is supplied to the grid.

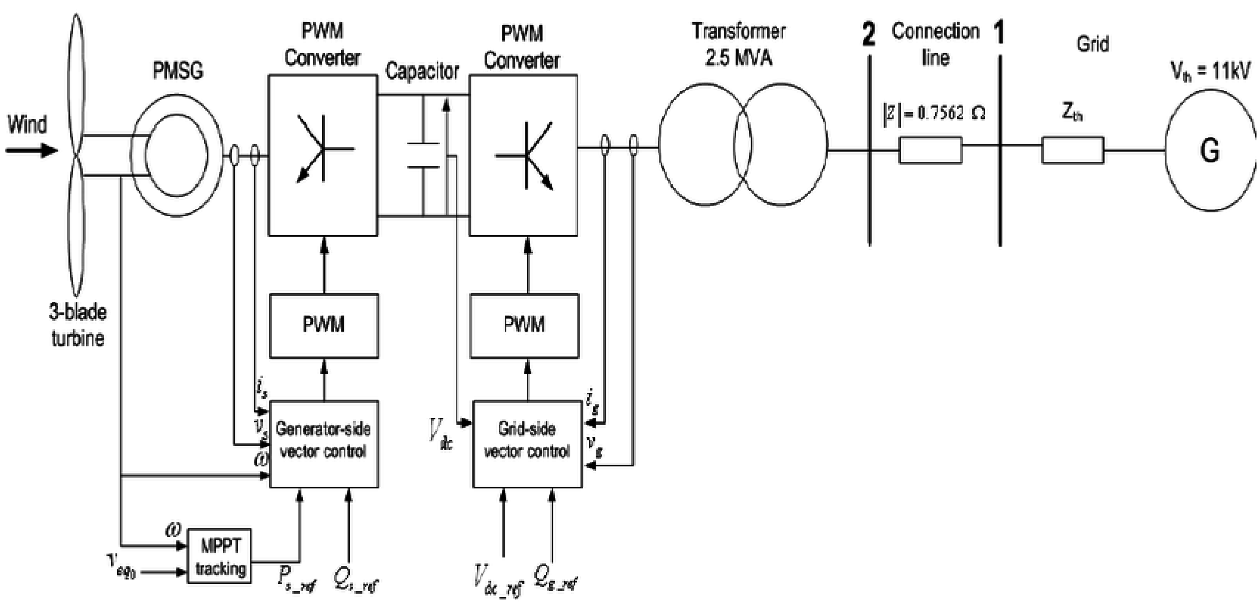

Figure 1: PMSG based wind power generation system schematic diagram. [4]

For this prethesis the task is limited to permanent magnet synchronous generator, generator side vector control system, the inverter loss system and the inverter parameter calculations only and the grid side vector control system, transformer connection and grid connection and control are out of scope.

The Simulink block diagram of the wind turbine system is shown in Figure 2 below. The wind turbine is connected directly with the generator. The shaft of the generator gets the rotational speed from the wind turbine block. The output torque of the generator is connected with the wind turbine block in order to control the torque of the wind turbine. In the right side of the figure different outputs like blade pitch status, wind speed, rotor power and generated power can be visualized graphically.

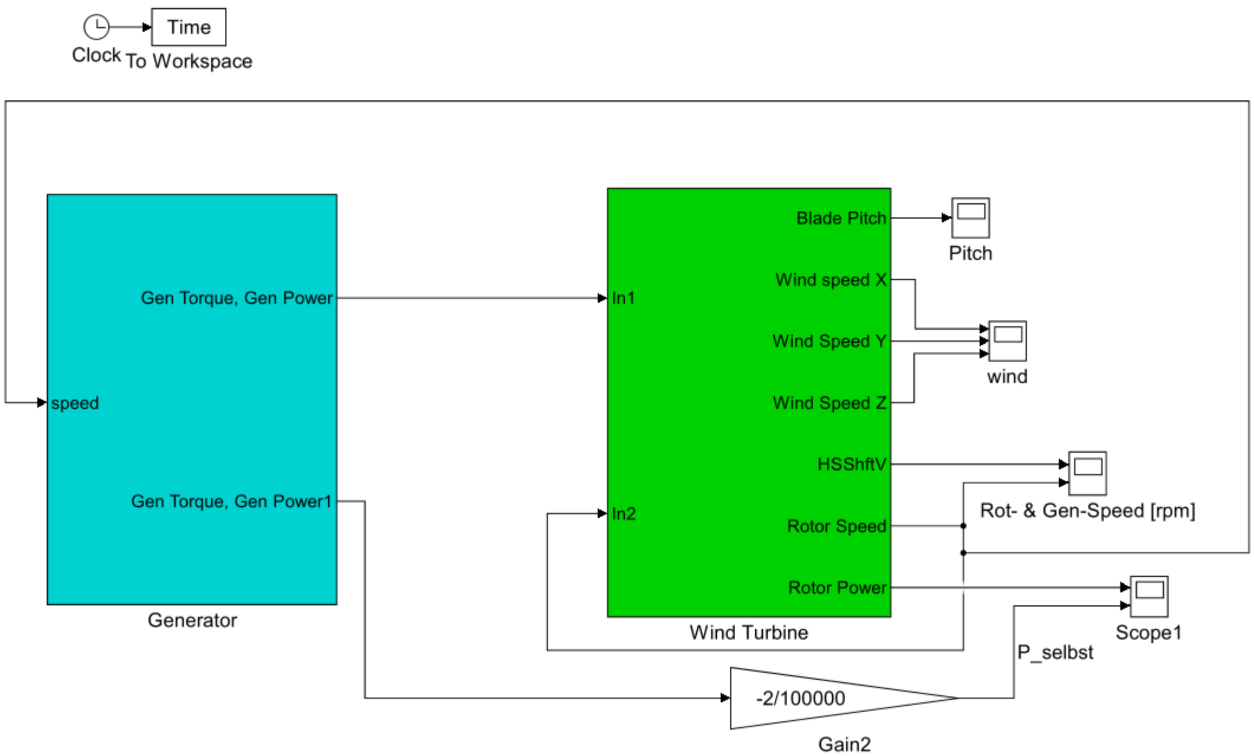

Figure 2: Simulink model of the wind power generation system

1.2 Wind turbine

The horizontal axis wind turbine of two or three blades are mostly used all over the world. The blades are mainly made of fiber or plastics while the tower are made of concrete or steel structure. The wind speed increases with the height. For this reason the taller towers are capable to extract more energy from the environment. The generated power from the wind can be approximated by the following equation [1]:

$$P = \frac{1}{2} * Cp * P * A * V^3$$

Where, P=extracted power from the wind, Cp=wind power coefficient, *P*=density of air, A=air passing through the area of wind turbine,*V*=wind velocity. The production of the wind power is changed with respect to the following parameters.

As mentioned earlier the generated power of the wind turbine changes with respect to the wind speed. The generated power from the wind is too low at lower wind speeds. On the other hand at higher wind speed the power is reduced by changing the aerodynamic torque. The wind speed vs the output power characteristics curve is shown below in Figure 3

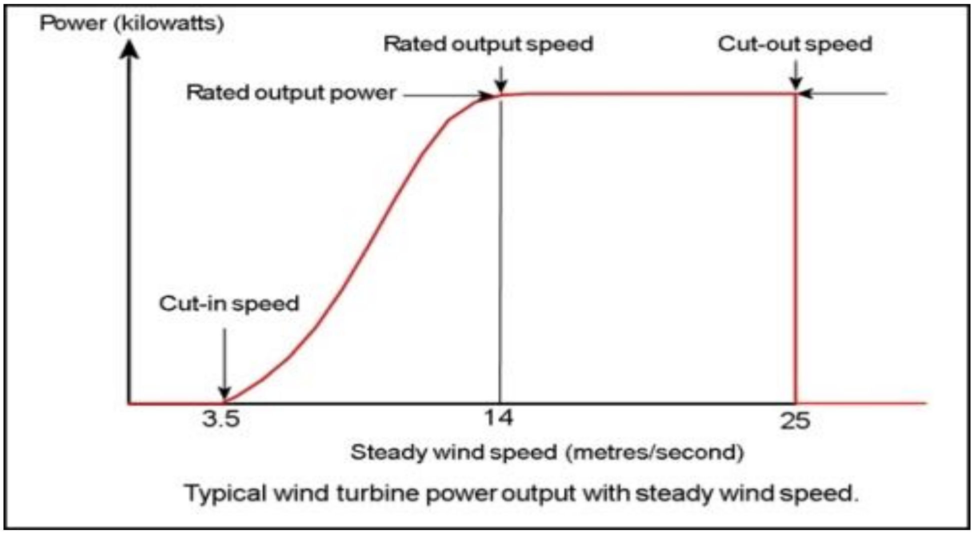

Figure 3: Typical wind speed vs power characteristics curve [5]

In order to control the output of the wind turbine three different kinds of control system are used in this simulation task: Yaw control system, pitch control system and high speed shaft brake

Figure 4 the control system yaw control, pitch control and the high speed shaft brake is shown while in the right side the gray box shows the different output scopes from the wind turbine: blade pitch,

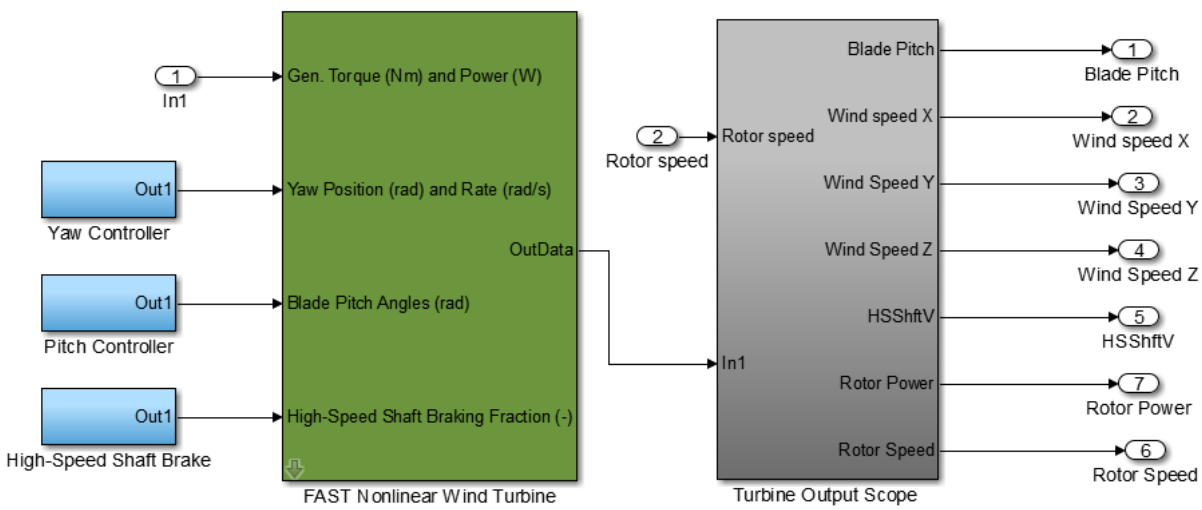

Figure 4 : Wind turbine and control system Simulink block

wind speed, rotor power, generated power etc. The green block in between them is the wind turbine. The matlab S-Function feature is used to build the wind turbine.

1.3 Wind Turbine Controller

Yaw controller

This controller is used to control the movement of the wind turbine nacelle in the direction of the wind. Typically yaw system mounted on the wind turbine senses the direction of the wind. In the Figure 5 of the Yaw controller the system is shown below. The yaw rate (radians per second) decides at which rate the turbine rotates in the direction of the wind. [6]

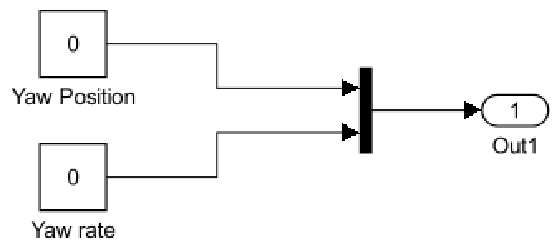

Figure 5: Simulink Yaw controller block diagram

Pitch Controller

This controller saves the wind turbine from overloading in the high wind speeds. At nominal wind speed the controller has approximately a zero value but as the wind speed increases above the rated value then the angle increases. [3]The Simulink control diagram for the wind turbine is shown in Figure 6

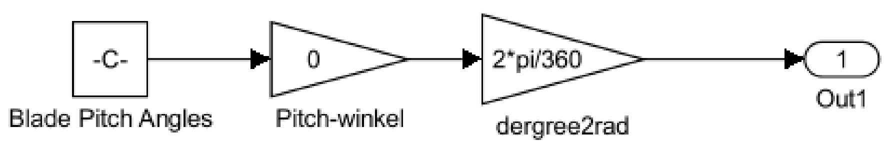

Figure 6: Simulink pitch controller block diagram

High speed shaft brake

This control system is responsible for the emergency braking and protects the turbine from gaining over speed. Generally, for high speed wind turbines this type of brakes are mounted on the generator side and on the turbine for low speed turbines. [7] Figure 7 shows the high speed shaft brake used in the Simulink model

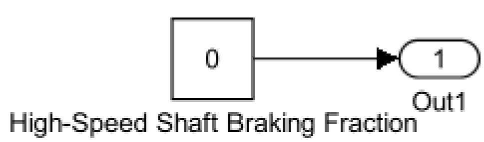

Figure 7: High speed shaft brake

2. Generator

The generator shaft is coupled with the rotor of the wind turbine. Since the wind turbine shaft rotates because of the wind disturbances the generator prime mover gets the rotational speed from the turbine and power is generated on the stator of the generator (indicated in Figure 8 below, right side colored in the cyan block). In order to control the torque, speed of the wind turbine and the currents a controller (indicated in Figure 8 below, left side colored in magenta) is mounted on the generator. The generator

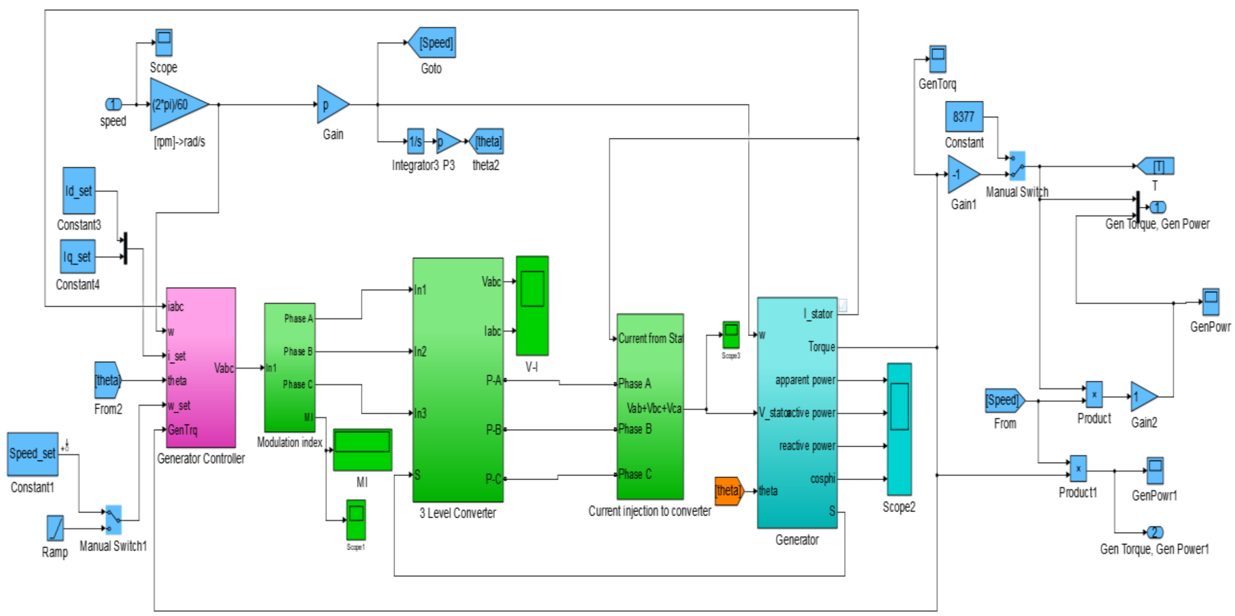

Figure 8: Generator block diagram includes converter (middle-green), controller (left-magenta) and generator (right-cyan) itself

controller output is fed into the generator via a machine side converter (indicated in figure 8 below, middle colored in green).Since the simscape feature of MATLAB is used for the converter it cannot be connected with the generator which is using the Simulink feature of MATLAB. In order to interface the two systems simscape and Simulink a current source (indicated by the color green as mentioned in figure 8 below) is used to synchronize the two systems. The whole Simulink model for the generator operation is represented in the Figure 8.

2.1 3 Level converter

Because of higher efficiency, lower losses, lower common mode voltage, lower voltage stress on power switches, lower (dv/dt) ratio, no EMI problems [8] and its sustainability for high voltage multilevel inverters are becoming more and more popular day by day. There are mainly three different types of multilevel inverters: Diode clamped (neutral clamped), Flying capacitor (capacitor clamped) and Cascaded H bridge multilevel inverters. [9]

2.2 Advantages of flying capacitor converter

Since there is no problem of voltage balancing issue in flying capacitor converter so it is an attractive choice. Flying capacitor converter practically does not suffer from voltage balance imposed performance limitations as opposed to multiple point clamped converter [10]. Voltage balance dynamics analytical research methods reported to date deal mostly with an AC modulation case and are essentially based on a frequency domain analysis using double Fourier transform. High mathematical skills are required to solve these methods and are difficult for engineers. [11]

2.3 Flying capacitor topology

,, The topology is called so because the capacitor's floats with respect to earth potential'' [12]. Sometimes it is also referred as capacitor clamped MLI (multilevel inverter). It is needed 2(m-1) main capacitors (dc link capacitors) and (m-1)*(m-2)/2 auxiliary capacitors (flying capacitors) in each leg in order to construct a m level flying capacitor MLI. Similarly, for this case of 3 level inverter it is needed 2 main capacitors and 1 auxiliary capacitor in each leg. [12]

A typical 3 level flying capacitor figure is shown below. It is seen from Figure 9 that there are four semiconductor switches S1, S2, S21, S11 and one free-wheeling diode in each switch. The switching mechanism is that if S1 is on then S11 is off and vice versa [13]. This idea is same for S2 and S21 while they are complementary to each other also.

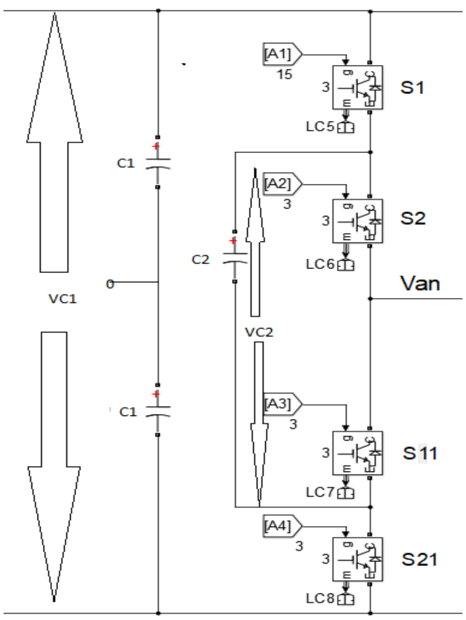

Figure 9: Single leg of a flying capacitor converter [14]

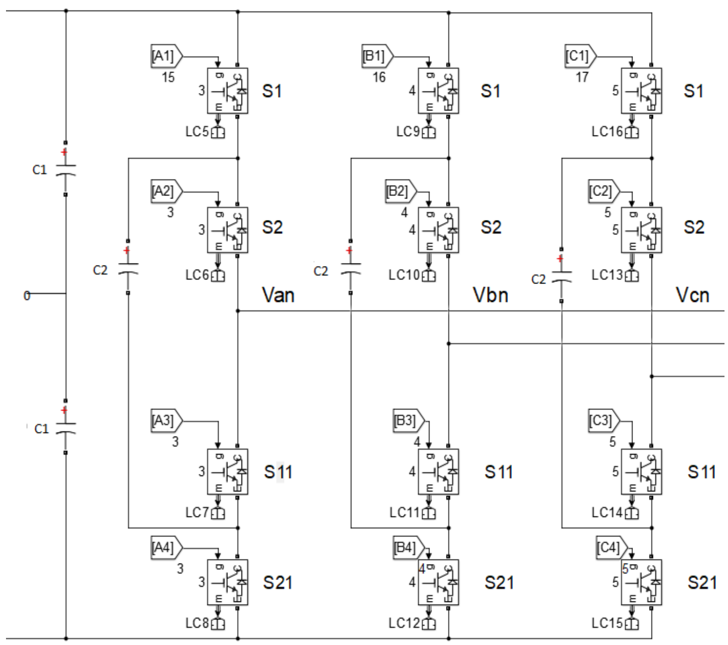

Figure 10: 3 leg of a 3 level flying capacitor converter [14]

Each capacitor (C1) shown in theFigure 9 is of equal voltage ratings. The capacitor C1 is charged externally by means by external sources. In 3 phase inverters there are two extra legs as shown in Figure 10. Every leg has a flying capacitor C2.Each flying capacitor does not depend to other flying capacitor. For example: If the initial voltage of phase A flying capacitor is Vdc then the voltage of the other flying capacitors of the other legs could be Vdc/2.In spite of that the system would work properly.

For any initial state of flying capacitor voltage the inverter output voltage is given by [15] [16] [9]

Van=S1 (Vc1-Vc2) +S2Vc2-Vc1/2

In the above equation when the switching combination S1 and S2 is conducting then the combination is equal to 1 but when they are not conducting then the combination is 0.The table below is summarizing the different combinations. State NC indicates that the capacitor is neither charging nor discharging and +, - indicates charging and discharging respectively. [11]

Table 1: Switching state and corresponding output of Phase leg A [17]

S1	S2	Van	C1
ON	ON	+Vdc/2	NC
ON	OFF	0	+
OFF	ON	0	-
OFF	OFF	-Vdc/2	NC

2.4 Modulation Strategy

SPWM method provides better output voltage and reduced order of harmonics. In order to make a m level inverter (m-1) level carrier waves are used. The frequency and the amplitude of the carrier waves must be same. The carrier waves are compared with the reference sine wave and the outputs of the comparators are then combined together and used to control the switches [18] [19]. The overview is shown in Figure 11.In the bottom of Figure 11, the generated switching signals are shown (pink color), which are applied to the switches. In the top part of the Figure 11 the two carrier wave (red and blue colored triangular wave) and the reference sine wave (gray color) is shown.

For 3 phase 3 level inverter 3 sinusoidal reference signals each displaced by 120° are compared with the carrier wave. The modulation index is given by-
Ma=Am/2*Ac

Where Am is the amplitude of the modulating signal and Ac is the amplitude of the carrier wave(P-P) . [20]

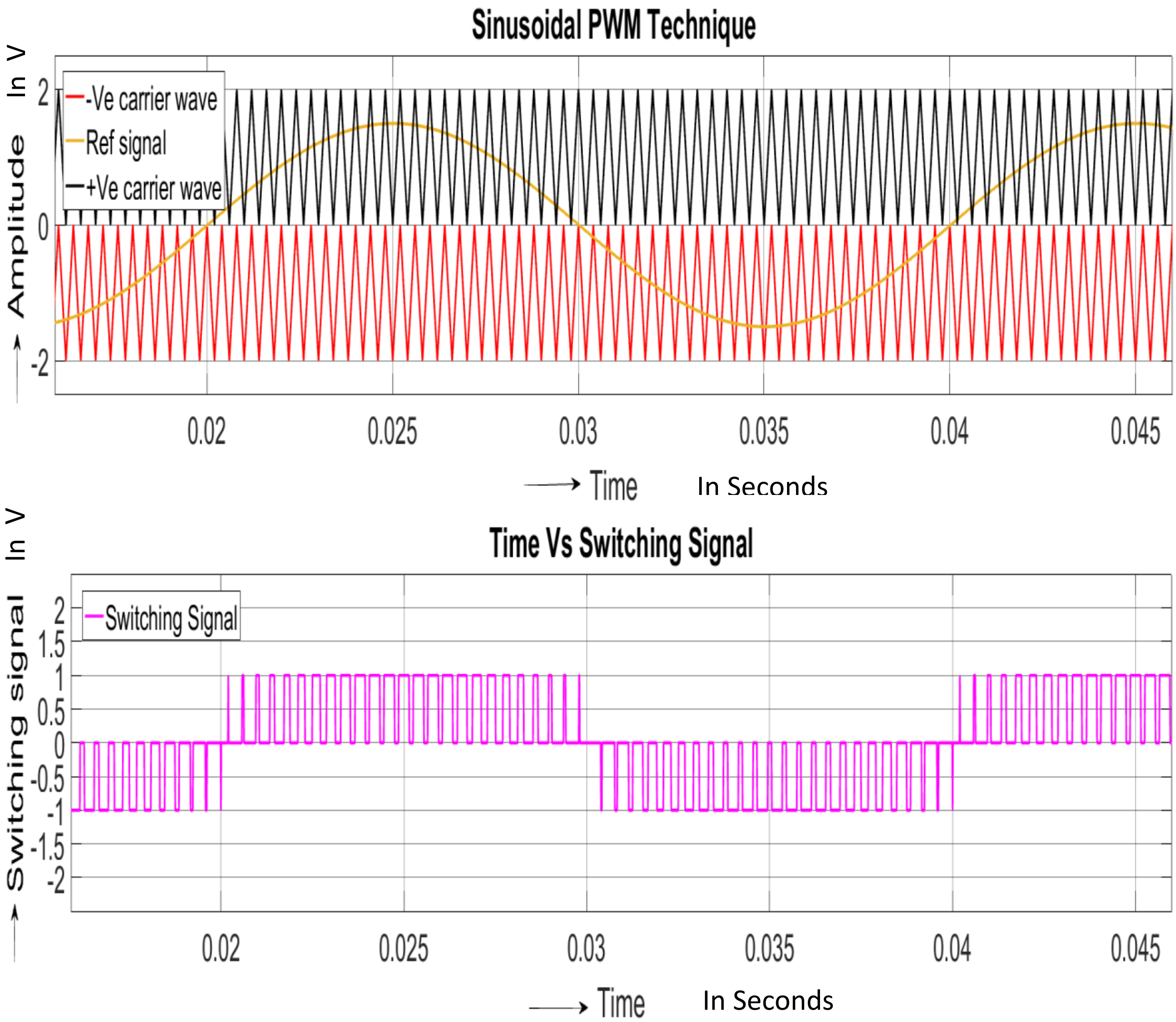

Figure 11: Carrier wave and reference signal (top), switching pulses (bottom) for single phase

2.5 Simulink block diagram of 3 level converter

The Simulink block diagram to connect the 3 Level converter with the generator is shown below in

Figure 12.In1, In2, In3 (mentioned in Figure 12 left side most) are the three reference signal which is to be used as the reference in the SPWM generator block. There are basically two parts of this 3 level inverter block: SPWM generator and the converter circuit. The SPWM generator block serves the purpose to generate switching signals for the switches of the 3 level inverter circuit. On the other hand the 3 level converter consists of two dc link capacitors and 4 IGBT switches in each leg. Three different colors are shown to indicate three different phases of the converter circuit. The output of the each phase is connected directly with generator which is

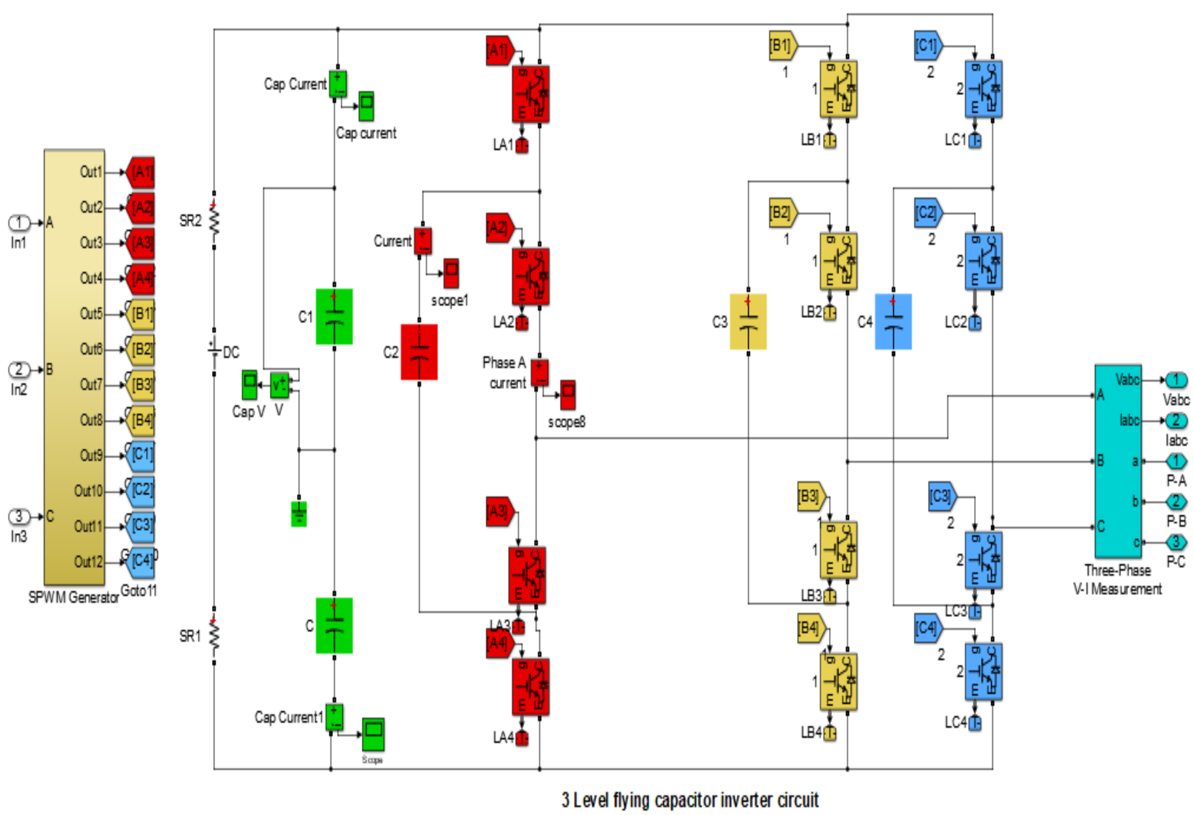

Figure 12: SPWM generator (left) and 3 level converter (right) block diagram

indicated in the figure: from each phase to point A,B,C(Three phase V-I measurement meter) respectively. There are three different flying capacitor connected with each phase. These capacitors are charged and floats to the neutral. The input pulses of the SPWM generator are denoted by A1,A2,A3,A4(Phase A),B1,B2,B3,B4(Phase B),C1,C2,C3,C4(Phase C) and are connected to each leg's switches' gate terminal.

The SPWM generator block as mentioned earlier that consists of two different sections: PWM signal controller for switches and Comparator section for generating switching signals shown in Figure 13(3 different colored sections for three phases).The comparator block compares a reference signal with carrier waves (of two level for three level converter) and generates pulsed signal for the switches. (Shown in Figure 14).

The reference signal is compared with a triangular wave(since a triangular wave has been considered here as a carrier wave) and if the magnitude of reference signal is larger than the triangular wave then the resultant output is 1 otherwise if less than the triangular wave then output is 0.Referred to Figure 11 this is graphically shown. In Figure 14 there are two carrier waves +ve and –ve .Since the converter being

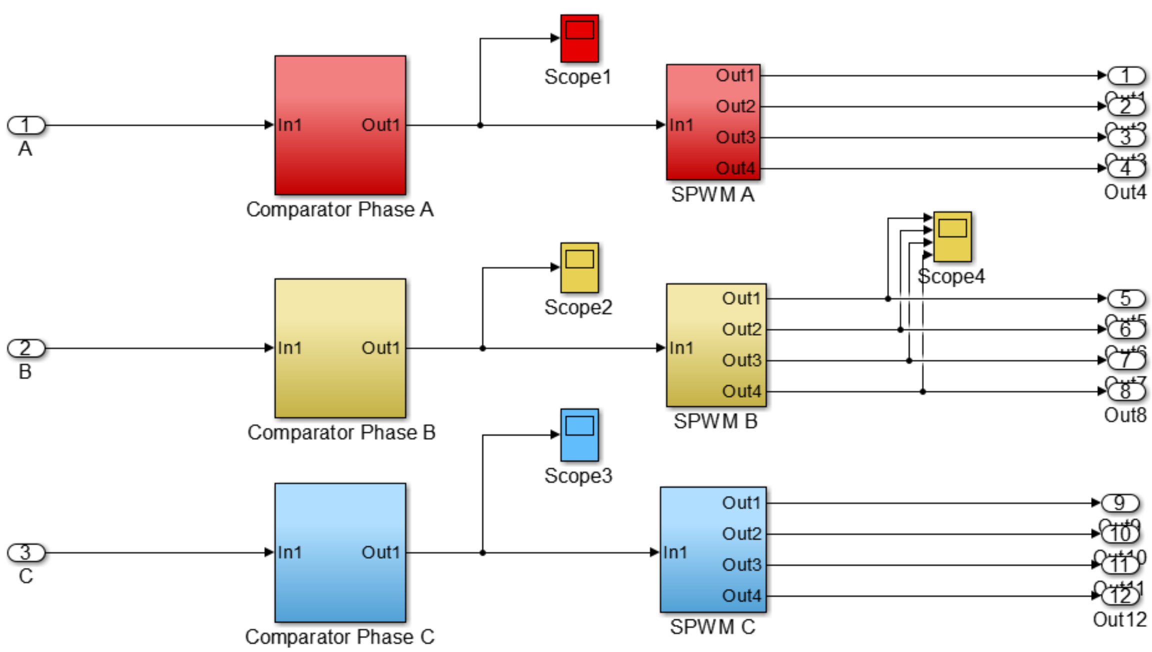

Figure 13: PWM controller (right) and Comparator block (Left)

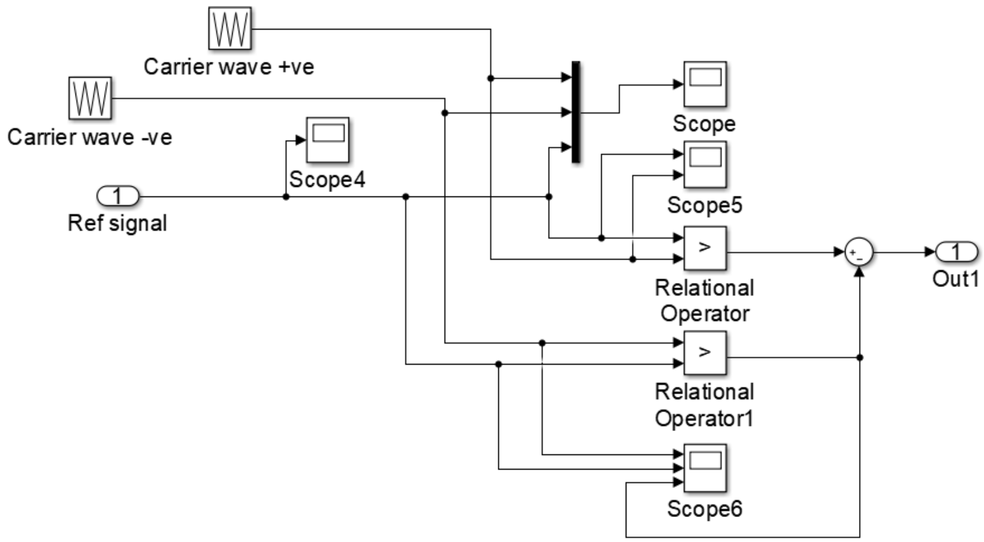

Figure 14: Comparator block internal architecture of SPWM generator

Used is a three level converter +ve carrier wave and –ve carrier wave both has to be compared with the reference signal in order to get the desired switching signal for 3 level converter(referred to Figure 11).

After generating the switching signals the next task is to input the switching signals (shown in Figure 17) to the desired switches. For this purpose a logic table is followed (shown in Figure 15) to give switching pulses to the switches of a particular leg.(shown in Figure 16).

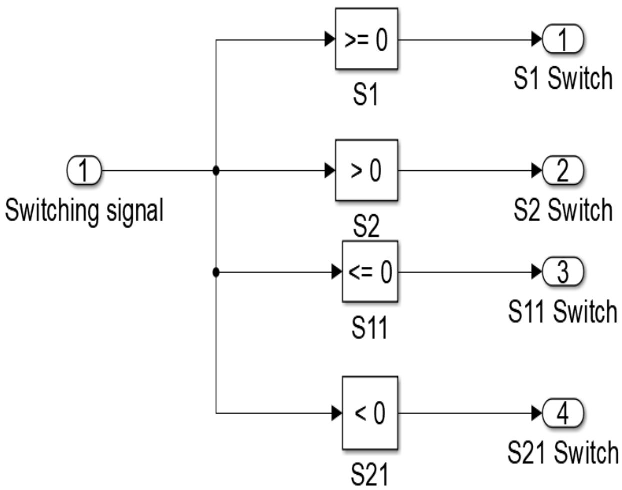

Figure 15: PWM controller block internal architecture.

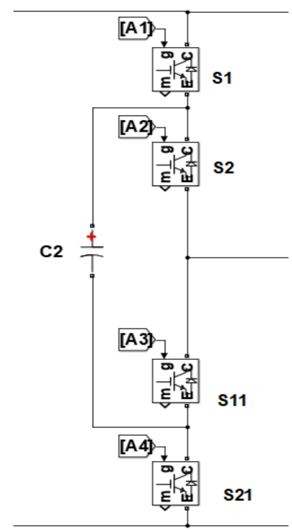

Figure 16: Switching signal input leg example.

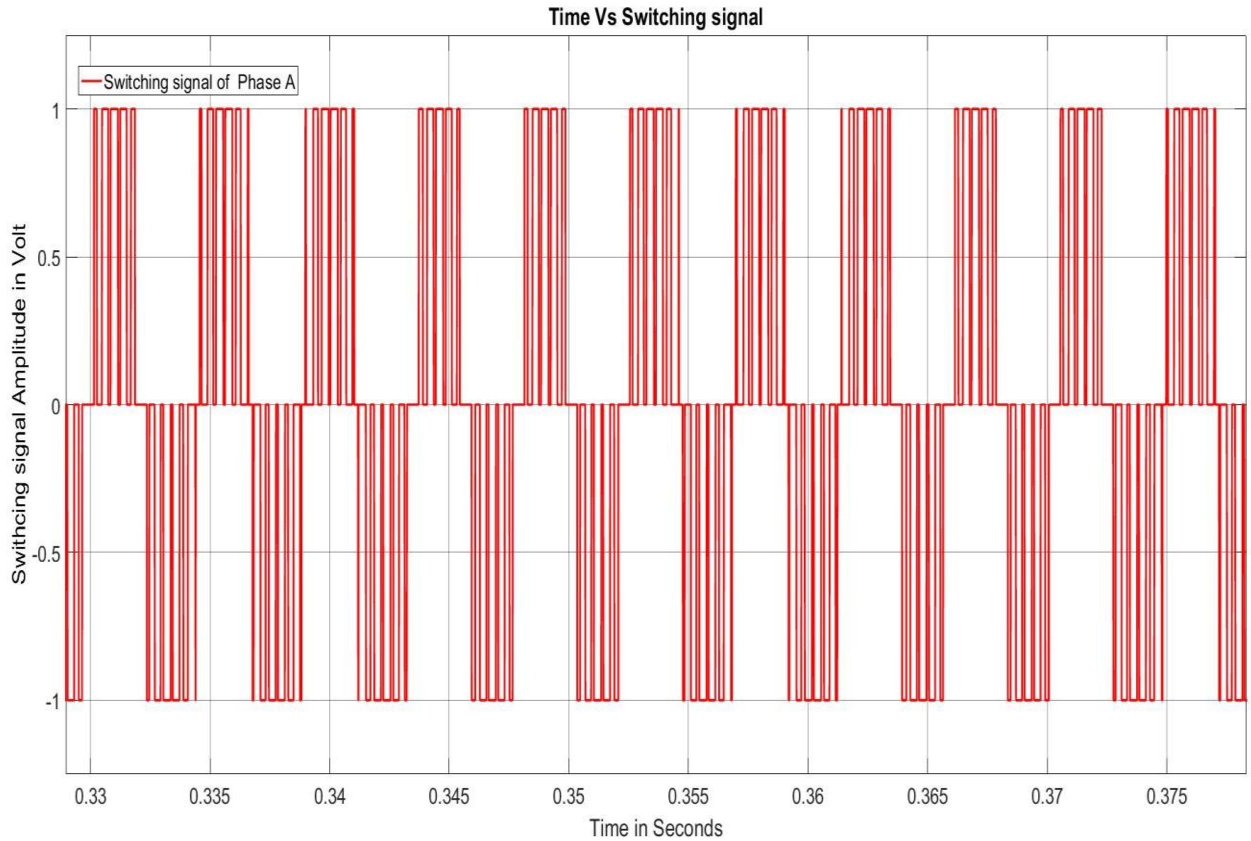

Figure 17: Switching signal from comparator.

2.6 Simulink block of instantaneous Modulation index calculator

In order to find the modulation index the ratio between the reference sinusoidal modulating signal to the carrier wave is taken.

The gain block (shown in Figure 18) minimizes the value of the modulating reference signal since the triangular carrier wave has a magnitude of 2V but the modulating reference signal has a magnitude of much higher values.

So first of all,abc to alpha-beta(Clarke transformation) was taken because the magnitude of the sinusoidal wave remains same. Then the Cartesian to polar block converts the alpha-beta wave to space vector. The magnitude of the space vector has the same as the magnitude of the reference sinusoidal wave.

Now, the ratio of the magnitude of the space vector and triangular wave were taken in the divide block which gives us the value of modulation index (shown inFigure 19).

The results were cross checked. First, the reference sinusoidal signal and carrier wave were manually taken from curves and the Modulation index was calculated. After that checked with the model output. There was no difference found.

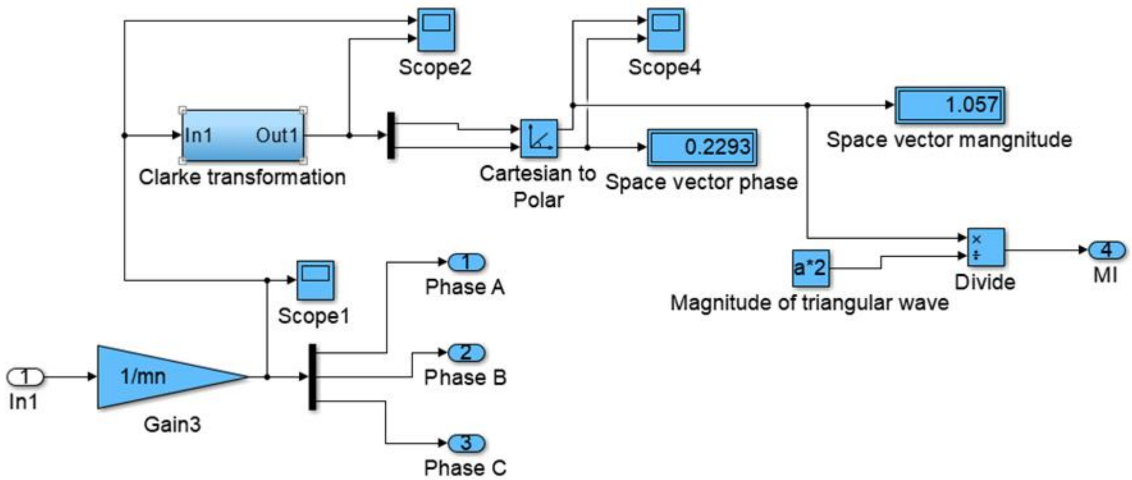

Figure 18: Modulation index calculating block.

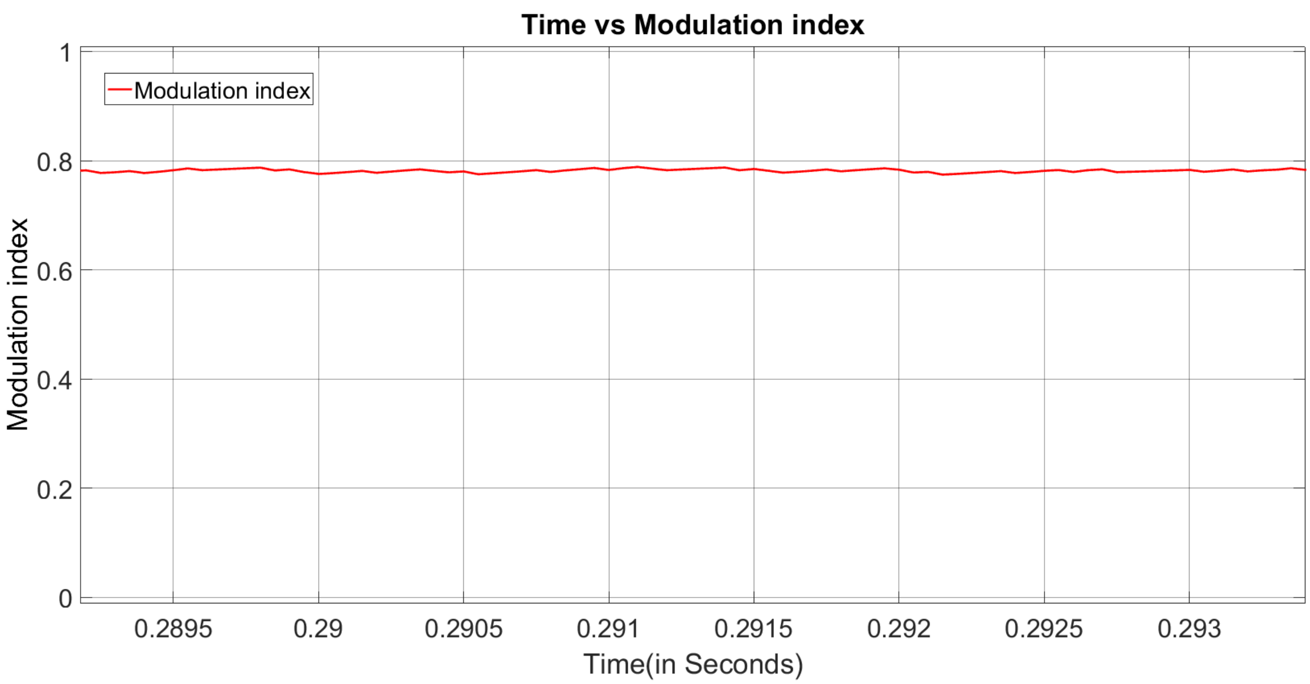

Figure 19: Modulation index vs time

3. Calculation of different components of the inverter system

The inverter system consists of flying capacitor, dc link capacitor, switches, switching frequency, modulation index for PWM methods. In this section the calculation of the dc link capacitors, carrier frequency, flying capacitor, switches, and modulation index will be explained in details:

3.1 DC link capacitor

Amplitude of the current ripple, permitted voltage variation, mean time between failures etc. these things are very much important in order to realize the size of a dc link capacitor. It helps the inverter to restrain from any kind of surges, momentary voltage spikes and EMI [21] . In a multi-level converter the purpose of this capacitor is to provide the energy between the delay times of the voltage variation. ,, The delay time can be estimated as the sum of the rise time of a rated step current response, filter delay time, and computation delay of the current response'' [22]. The backup energy can be approximated as

$$\Delta Wdc \geq \frac{\Delta Pmax * Tr}{2} \text{ .... } (1)$$

Where Tr is the delay time, ΔW_{dc} =energy to be stored in the capacitor. The voltage fluctuation for this is –

$$\Delta Vdc \geq \frac{\Delta Wdc}{Cd * Vdc} \text{ .... } (2)$$

Where ΔPmax is the load variation, ΔV_{dc} is the voltage fluctuation. If the value of ΔW_{dc} from equation (2) is given input to equation (1) then the capacitor value becomes –

$$Cd \geq \frac{\Delta Pmax * Tr}{2 * \Delta Vdc * Vdc} \text{ .... } (3)$$

The resulting equation is including a >= because we can choose the equal or the larger value but not less than that value. In market there will not be exact capacitor value as in our calculation so we can buy larger than that. [22]

Let us consider our case as an example:

Back up calculation of time:

The following data has been taken from reference [23] for back up time calculation:

Table 2: Back up time calculation data

Variable Name	Variable Notation	Value given
Back up time	Tr	to be calculated
DC link voltage	V_d	600V
Rated power	ΔPmax	1.5MW
DC link capacitance	Cd	.5F

Since the voltage fluctuation considered here for capacitance calculation has not been mentioned. So, we have to use a different formulae of capacitor's stored energy calculation. The energy which can a capacitor store is-

$$W = \Delta\text{Pmax} * \text{Tr} = \frac{1}{2} * Cd * V_d^2$$

If we put all the values in the above equation then the value of Tr found is .06s.

Table 3: DC link voltage calculation data [23]

Variable Name	Variable Notation	Value given
Back up time	Tr	.06s**
DC link voltage	Vd	600V
Rated power	Δpmax	1.5 MW
DC link capacitance	Cd	To be calculated
Voltage fluctuation	ΔVdc	150V
**In order to find this time back calculation method is used in reference [23]		

If all the values are put in equation 3 then the value of capacitance found is 0.5F.

The DC link capacitor voltage charging and discharging curve is shown in Figure 20

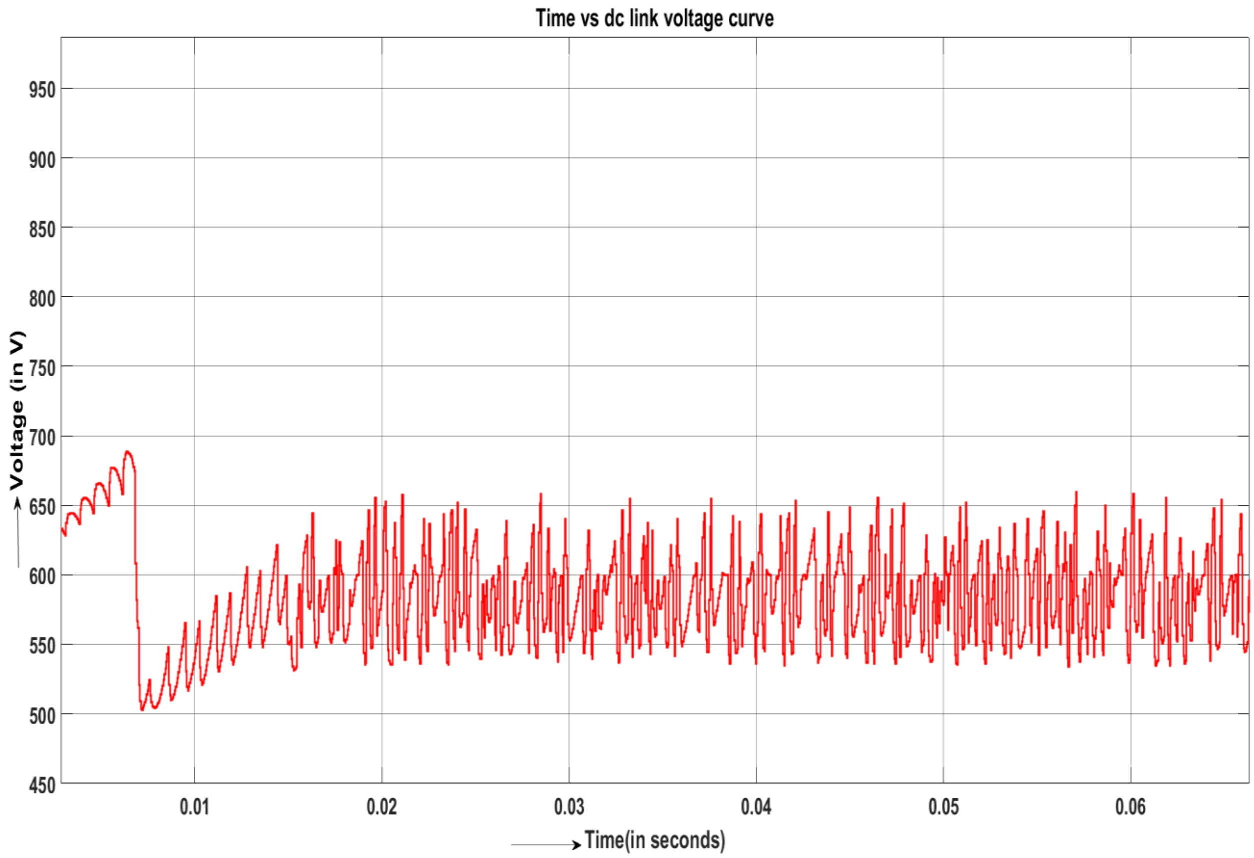

Figure 20: Time vs DC link capacitor voltage

3.2 Carrier frequency Selection

The switching loss decreases with the reduced switching frequency. The reason behind is that at reduced switching frequency there are lower number of sampling points. Lower number of sampling point means lower number of switching transitions and for this reason it causes lower switching loss.

However, lower number of switching frequency increases the THD due to increased notches within the width of each generated output pulse. [24]

To find out the optimum frequency for the inverter Phase A voltage is taken as a reference here. At first the frequency is taken 500 Hz and the corresponding switching loss, THD values are taken from model. After that the frequency is increased gradually at 500 Hz interval and the corresponding values are taken. The data found during the experiment is summarized below in the table.

Table 4: Frequency vs THD and switching loss

Frequency(in Hz)	500	1000	1500	2000	2500	3000	3500	4000	4500	5000
THD(in %)	29.03	45.25	48	32.1	17.58	34.04	24.04	29.98	30.58	35
Switching loss(in KW)	.8173	.8592	.90	.92	.8278	.9195	.8985	.9249	.93	.9229

After finding the values the next task is to plot the losses and the THD values in a diagram (shown in Figure 21). From the diagram the optimum point is calculated. The optimum point is that point where the switching losses and THD values have lower values and lower ratio. For this task the optimum point is found at 2500Hz.

Figure 21: Switching loss and THD vs frequency plot

3.3 Flying capacitor

In order to get the multilevel output(shown in Figure 25 below, the output voltage has 3 different levels, at 0V,500V and 1200V.By using these three level a sinusoidal wave is approximated which is the purpose of multilevel converter.

By the dc link capacitors the flying capacitors should be charged at their rated values [17] .The capacitance values of the flying capacitors should be selected in such a way that they can be charged by the dc link capacitors during the switching period of the inverter. The charging characteristics of flying capacitor is shown in Figure 22.

The rated voltage for the dc link capacitor is 600V,the time constant value should be such that the dc link capacitor can charge the flying capacitor to .637*600V=382.2V. The capacitance value should be selected in such a way that it should charge the flying capacitor to the desired voltage in that particular switching period. From the charging equation of capacitor [25]-

$$V_c = V_s(1 - e^{\frac{-t}{RC}}) \text{ ....(1)}$$

Where,

V_S=the source voltage which is charging the capacitor, here it is 600V.

V_C=The voltage across the flying capacitor, here it is 63% of the source voltage.

t=The time to charge the capacitor, it is invert of frequency.

R=resistance value present in the charging circuit, here it is .02 Ohm.

C=the capacitor value which is to be found.

If all the values are put in the above equation then the calculated value of the capacitance value is found .02 F.

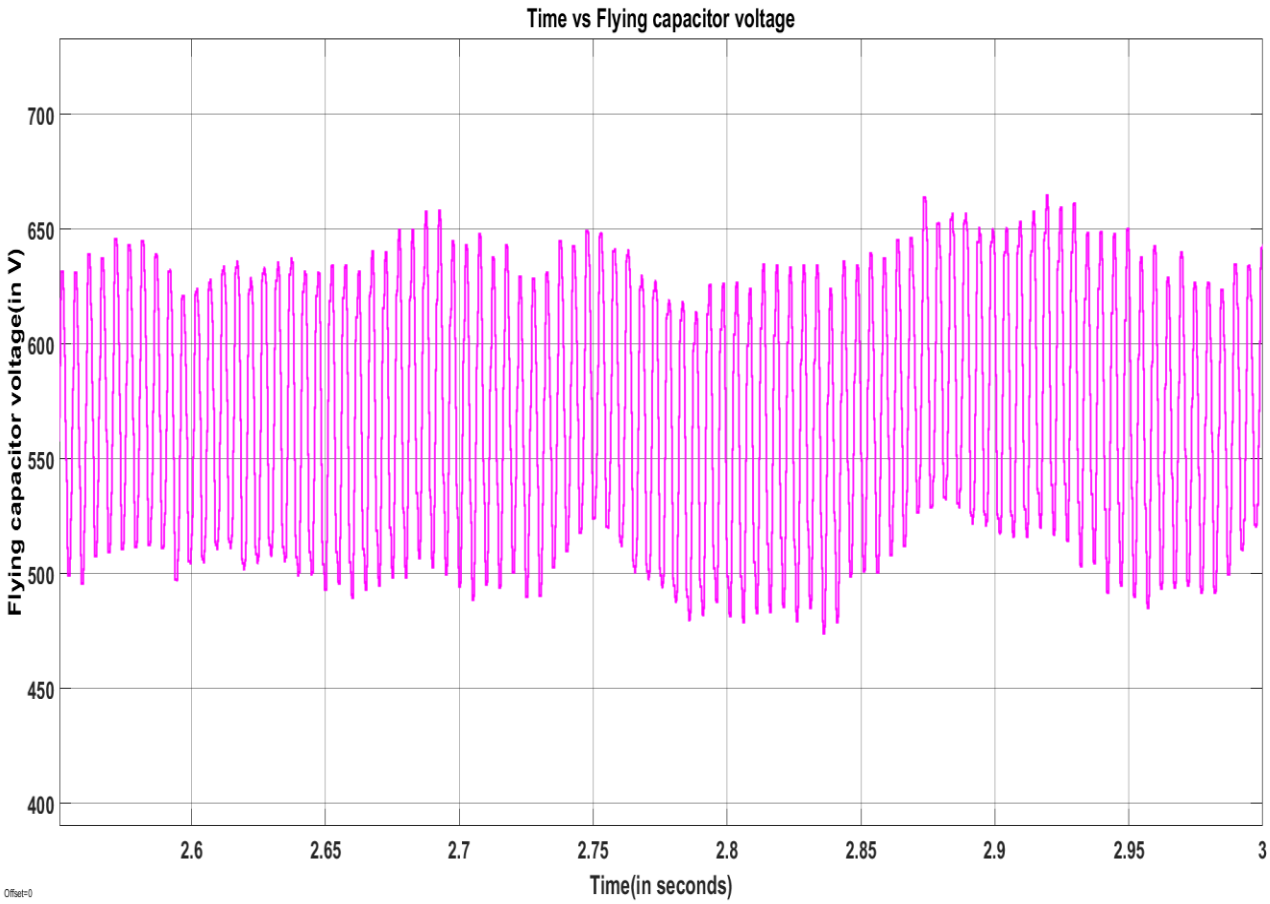

Figure 22: Time vs flying capacitor voltage

3.4 Modulation index

Referred to section 2.4 Modulation Strategy the modulation strategy was explained. In this section the optimum modulation index for this system is calculated. In order to calculate the optimum modulation index phase A is taken as a reference phase. The switching frequency is set to 2500 Hz and the simulation is observed till 1s.The modulation index was changed and the corresponding data of THD is taken. Based on the lower value of THD the optimum value of modulation index is selected.

The modulation index vs THD table is shown below and the corresponding variation is plotted (shown in Figure 23) to find out the optimum point.

Table 5: Modulation Index vs THD

Modulation index	1.55	.83	.769
THD (in %)	11.34	7.72	9.36

The optimum value for modulation index is chosen as .83(shown in Figure 23)

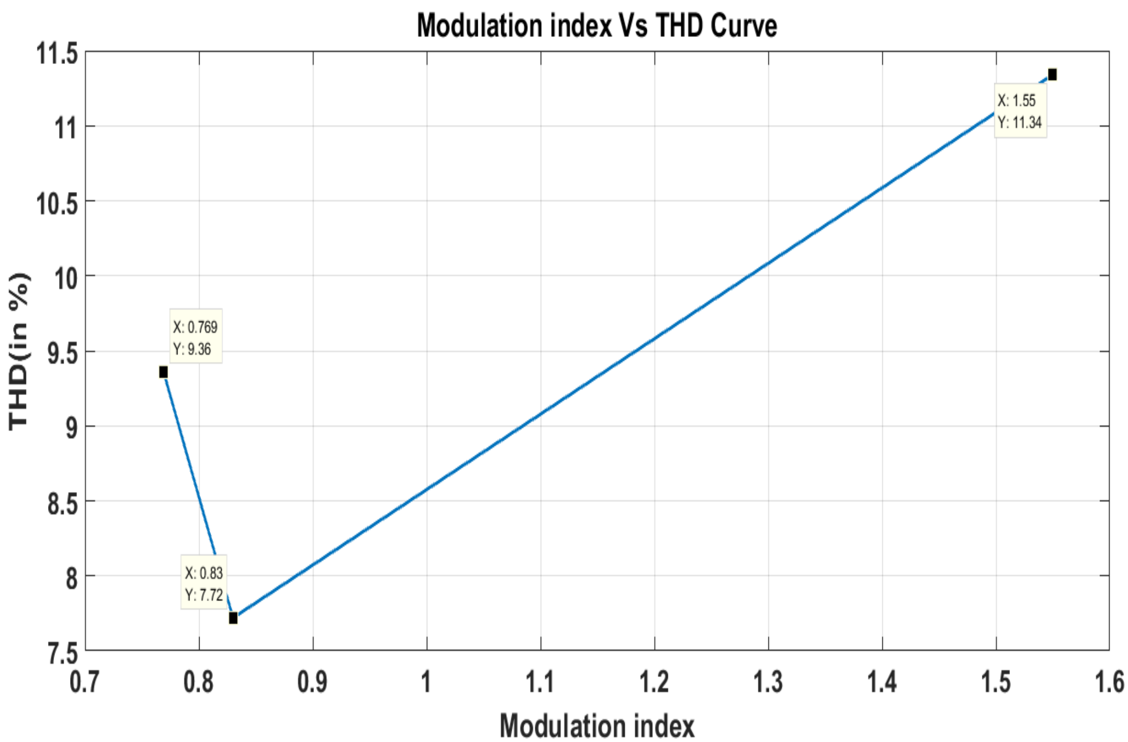

Figure 23: Modulation index vs THD Curve

3.5 Switches

The selection of MOSFET and IGBTs depend upon some criteria. For lower duty cycle, low frequency application and high power application IGBT is chosen while the MOSFET is suitable for high frequency and low power applications. Particularly below 5 KW application MOSFET is used and above this value IGBT is preferred. [26]

In the Figure 24 below the relative selection process is shown graphically. In the left side of Figure 24 it summarizes the selection process of a switch based on current and voltage. For example the maximum voltage and current rating of MOSFET are 1000V and 700 A respectively. The maximum current and voltage rating for IGBT are 7200A and 6500V.

In the right side of Figure 24 it shows the selection process based on voltage and frequency. For example

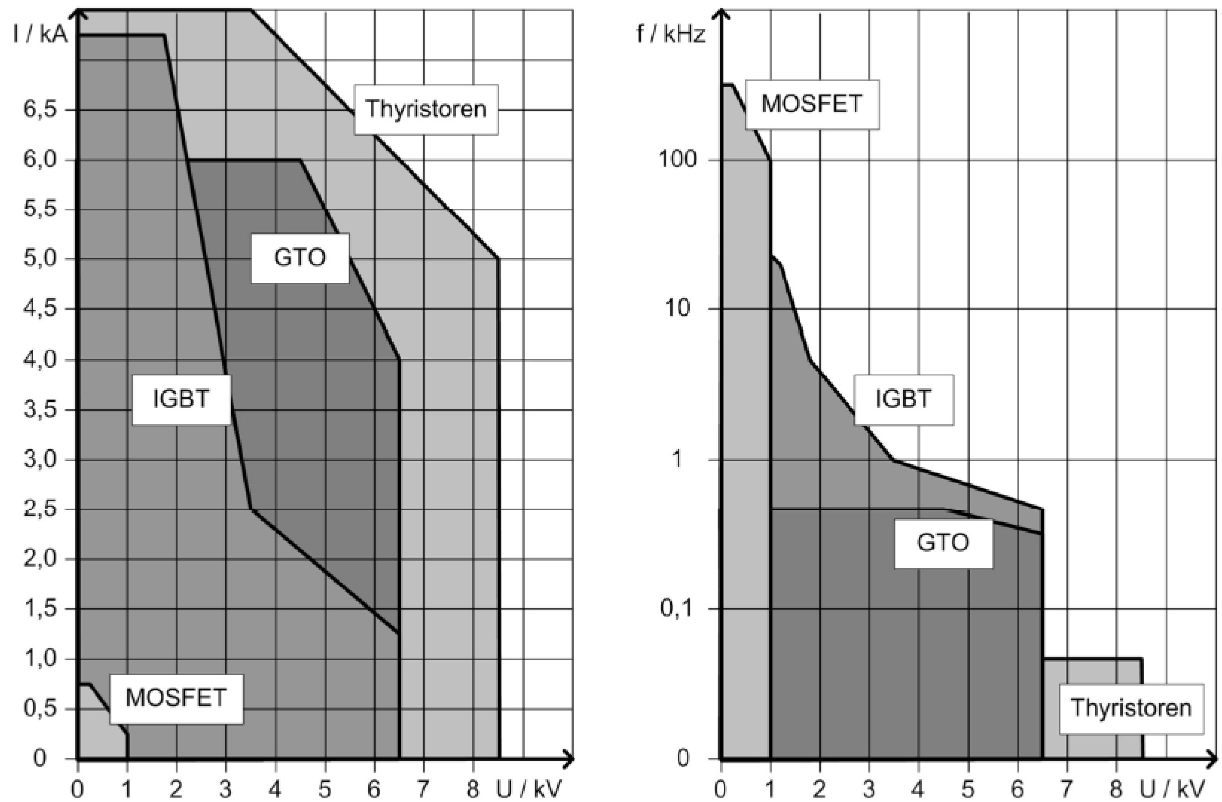

Figure 24: Comparison of MOSFET and IGBT selection [27]

the frequency and voltage range of MOSFET are 110KHz and 1000V approximately. Meanwhile the corresponding values for IGBT are 15KHz and 6500V.

.For this inverter system that is being designed the frequency range is 5KHz,the voltage, current values are 600V,3000A and the three phase power rating is around 1.5MW.MOSFET cannot be selected here. So, IGBT is the best choice for this application.

3.6 Simulation result of a 3 level converter

In order to simulate the output of a 3 level converter sinusoidal wave is considered as the reference signal as shown in the

Figure 12 the carrier wave frequency (triangular wave with 2500 Hz).The resultant line to line voltage is shown in the Figure 25 below.

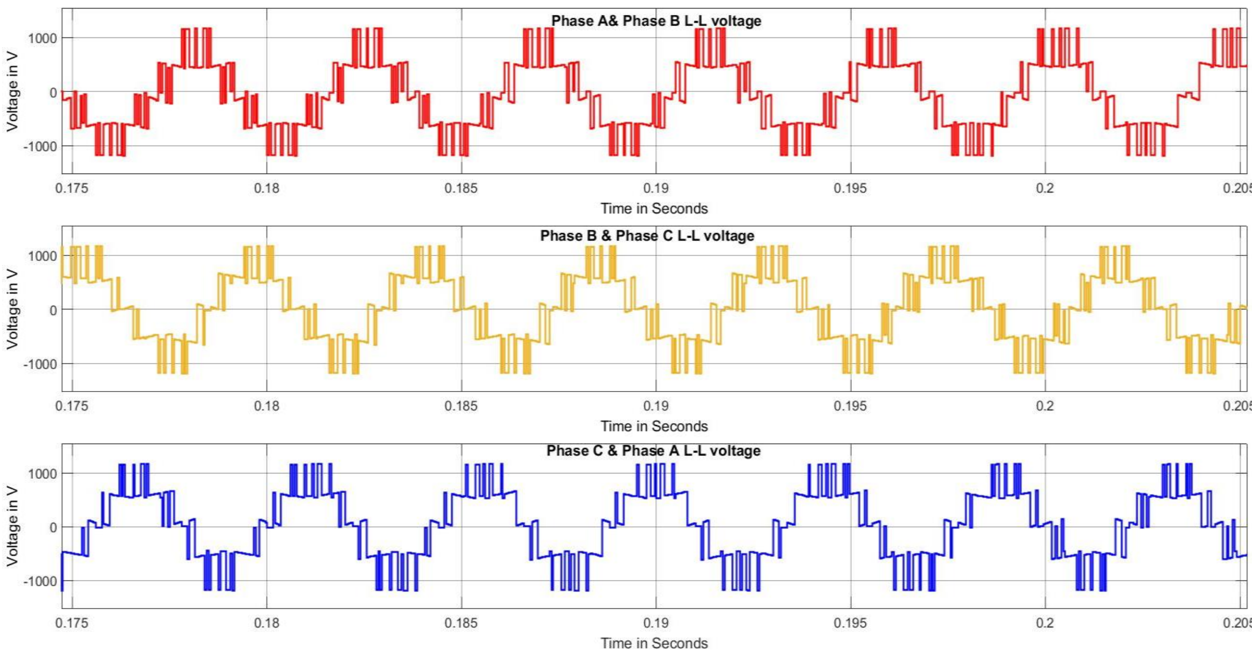

Figure 25:3 level L-L voltage output.

3.7 Current injection to the converter

The generator simulated in this model are created by using the MATLAB Simulink feature while the 3 level converter is simulated by using the simscape feature. The simscape feature is the physical model system. The direct connection between the two systems is not possible. In order to synchronize the two systems current sources have been interacted as shown in Figure 26.

Because of the rotation of the rotor of the wind turbine there is a generated voltage in the stator of the generator and a stator current is available on the output. This stator current is given as the input to the current sources which is connected in the a,b,c phases(red, yellow and blue colors for Phase A,B,C respectively) of the 3 level converter(shown in fig 24). So, the current which is flowing in the stator of the generator is virtually flowing in the converter also. The diagram is shown in fig 24.The relative comparison of the converter current (after introducing current sources) and the stator current is shown inthe

Figure 27.

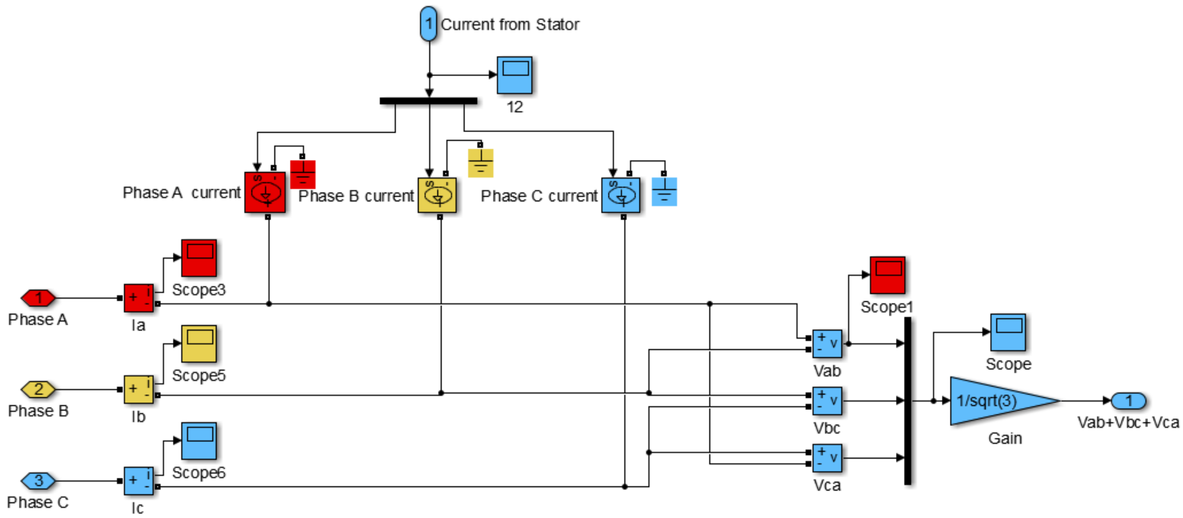

Figure 26: Current injection to the converter block internal architecture

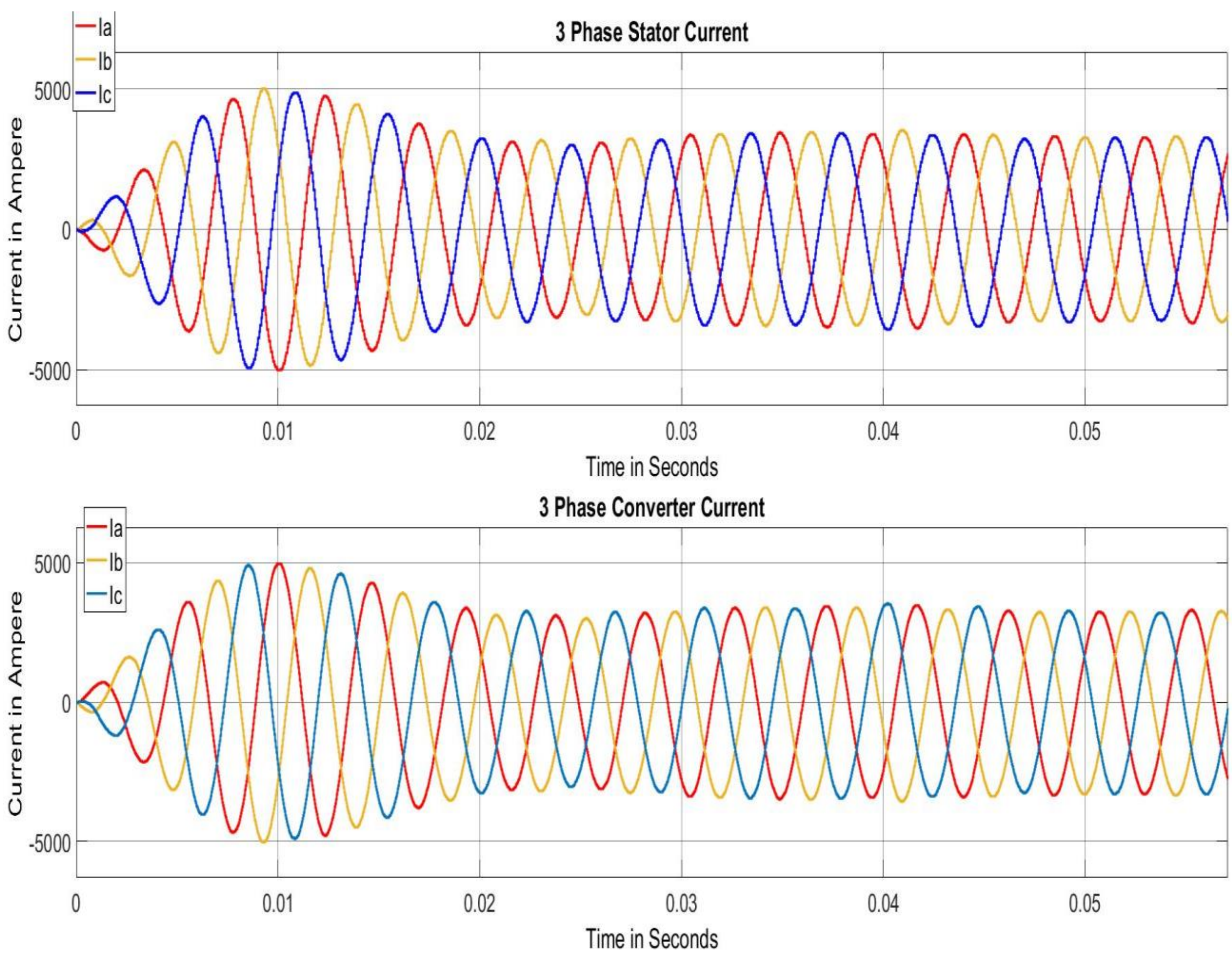

Figure 27: 3 Phase stator current and converter current

4. IGBT and Diode losses calculation

Since the power rating is 1.5 MW and the frequency range is around 3 KHz,the switching device chosen for this application is IGBT.

IGBT and Diode power losses in any semiconductor device can be divided into three types.

a) Conduction losses (Pcond): When the device is conducting then the energy which is dissipated as heat is called conduction losses.

b) Switching losses (Psw): During switching ON and OFF the device has some losses. It is called switching loss.

c) Blocking losses: When the device is fully OFF then the losses due to this phenomenon is referred to as blocking losses. But generally this loss is neglected in comparison to the other losses involved. [28] [29]

Therefore,

Ptotal = Psw+ Pcond+ Pb≈ Psw+ Pcond

4.1 Conduction Losses Calculation

Before calculating the IGBT conduction losses the following formulae is approximated [30]-

$$u_{CE}(ic) = U_{CEO} + r_C * i_C$$

Where,
U_{CE} = forward voltage drop
U_{CEO} = IGBT on-state zero-current collector-emitter voltage
r_C = collector emitter on-state resistance
i_C =Collector current.

For diode conduction losses it is approximated in the same way. The equation is represented below [28]:

$$U_D(i_D) = U_{D0} + r_D * i_D$$

Where,
U_D =Diode forward voltage drop
U_{D0} = Diode on state voltage
i_D = Diode current.
r_D = Diode on-state resistance.

After the approximation of the formulae the instantaneous value of the IGBT conduction loss is [30]:

$$P_{CT}(t) = U_{CEO} * i_C + r_C . i_c^2$$

Where,

P_{CT} (t)=instantaneous conduction loss of IGBT.

The average losses can also be expressed in the following equations [28]:

$$P_{CT} = U_{CEO} * I_{cav} + r_c * I_{crms}{}^2$$

Where,

I_{cav} = the average IGBT current value

I_{crms} = the rms value of IGBT current

The instantaneous value of the diode conduction losses is [28]:

$$P_{CD}(t) = U_{DO}(t) * i_D(t) + r_D * i_D^2(t)$$

The average losses can also be expressed in the following equations: [28]

$$P_{CD} = U_{DO} * I_{Dav} + r_c * I_{Drms}{}^2$$

I_{Dav} = the average diode current value

I_{Drms} = the rms value of diode current

4.2 Switching losses Calculation

The turn-on energy losses in IGBT (E_{onT}) can be calculated as the sum of the switch-on energy without taking the reverse recovery process into account (E_{onTi}) and the switch-on energy caused by the reverserecovery of the free-wheeling diode (E_{onTrr}) [30]:

$$E_{onT} = \int_0^{tri+tfu} u_{CE}(t) * i_c(t)dt = E_{onMi} + E_{onMrr}$$

The peak of the reverse-recovery current can be calculated as:

$$I_{Drrpeak} = 2*Q_{rr}/trr$$

Turn-on energy in the diode consists mostly of the reverse-recovery energy (E_{onD}) [30]:

$$E_{onD} = \int_0^{tri+tfu} u_D(t) * i_D(t)dt = E_{onDrr} = Q_{rr} \cdot U_{Drr}/4$$

Where, U_{Drr} is the voltage across the diode during reverse recovery. For the worst case calculation this voltage can be approximated with a supply voltage. The switch off energy losses of the diode are normally neglected. Therefore [30],

$$E_{offT}=\int_0^{tri+tfu} u_{CE}(t) * i_c(t)dt$$

The switching losses in the IGBT and the diode are the product of switching energies and the switching frequency(fsw) [30]:

$$P_{swM}=(E_{onM}+E_{offM})*f_{sw}$$

$$P_{swD}=(E_{onD}+E_{offD})*f_{sw} \approx E_{onD}.f_{sw}$$

4.3 Simulink Block for losses calculation

In the IGBT there are four connecting points to connect it to the system. The output from the m point (shown in Figure 28) contains two signals: currents and voltages of the IGBT and diode. Later on a demultiplexer is used to separate the voltages and currents. These currents and voltages drop is used to calculate the IGBT losses. In Figure 29 the outputs are taken by using 4 goto blocks LA1, LA2, LA3,LA4 for leg A and LB1,LB2,LB3,LB4 for leg B and LC1,LC2,

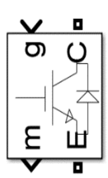

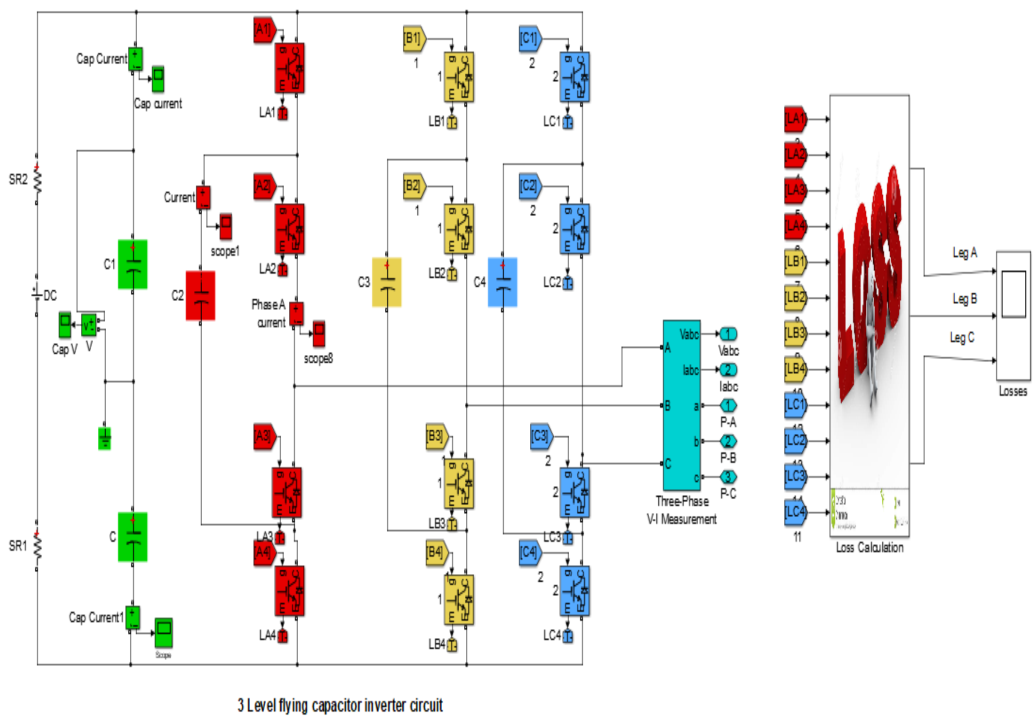

Figure 28: IGBT block [31]

Figure 29: Switching loss and conduction loss calculation block

LC3,LC4 for leg C respectively. The red, yellow and blue color (shown in Figure 29) represent Phase A, Phase B and Phase C successively. The voltage and current information is sent to the loss calculation block (right of Figure 29) for loss calculation.

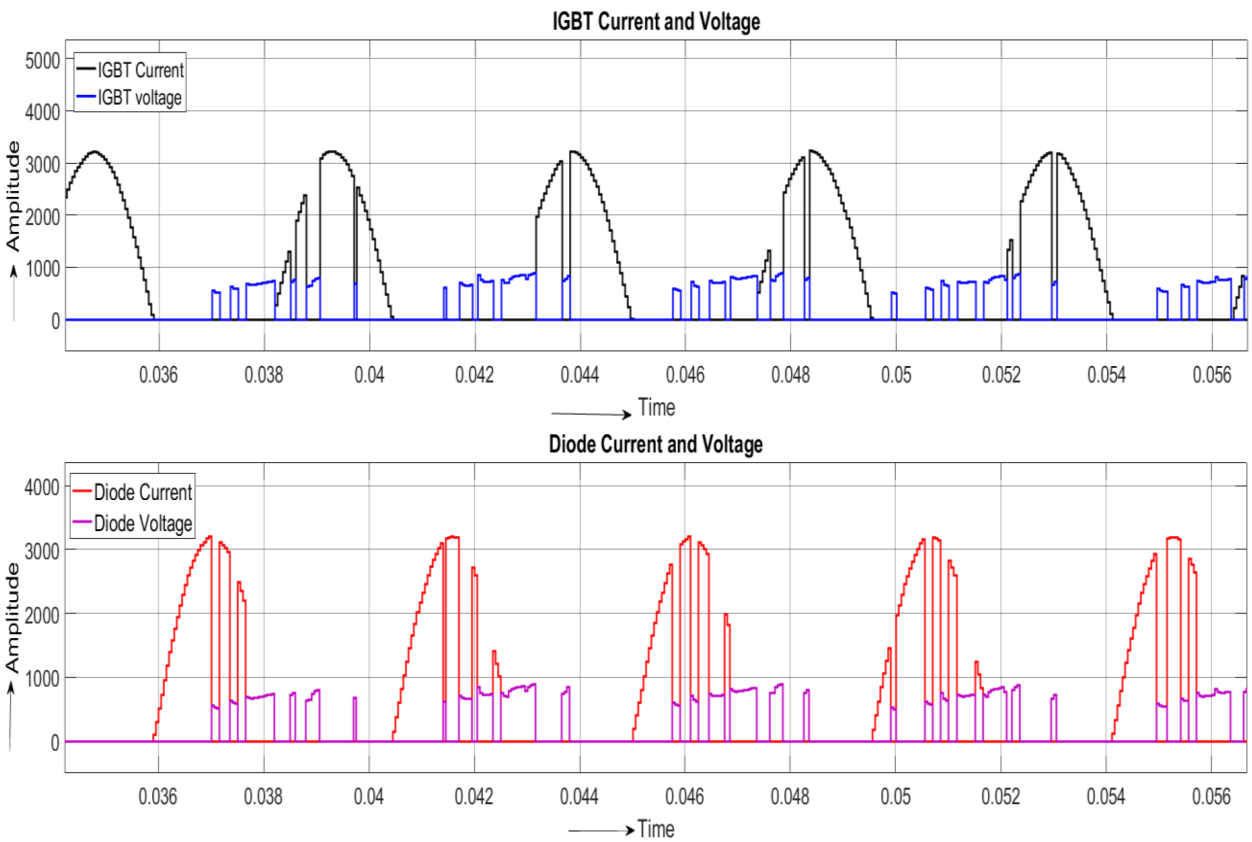

Figure 30: IGBT and diode current (in A), voltage (in V) graph to calculate the losses vs Time (in Seconds)

4.3.1 Conduction and switching loss model overview

After getting the current and voltage information from the m point of the IGBT the voltages and currents of IGBT and diode are demultiplexed in the demultiplexer block (shown in Figure 31,left side green block).Then,the individual current and voltage of IGBT and diode are sent to upper block(colored in magenta, named as IGBTs losses calculation) for IGBTs loss calculation and in lower block(colored in cyan, named as diodes losses calculation) for diode losses calculation shown in Figure 31.

The next task after loss calculation is to simulate the temperature rise due to losses of IGBT and diode which is done immediately after the loss calculation block in ,,Thermal model'' block(colored in red, right side of Figure 31).After the temperature rise calculation, this information is sent to the ,,Heat flow source'' block (the right side of Figure 31 colored light blue).The output of ,,Heat Flow Source'' generates a physical signal for simscape block(since the heat flow calculation is not possible to simulate in simulink) named ,,heat sink''.The heat sink block will be explained later in detail of this part. There are two small blocks named ,,ZO'' and ,,PS'' used between heat flow source block and thermal model block. The purpose of ,,ZO'' is to synchronize the information exchange between the Simulink and simscape system while the purpose of ,,PS'' block is to generate a physical signal from a simulink signal.

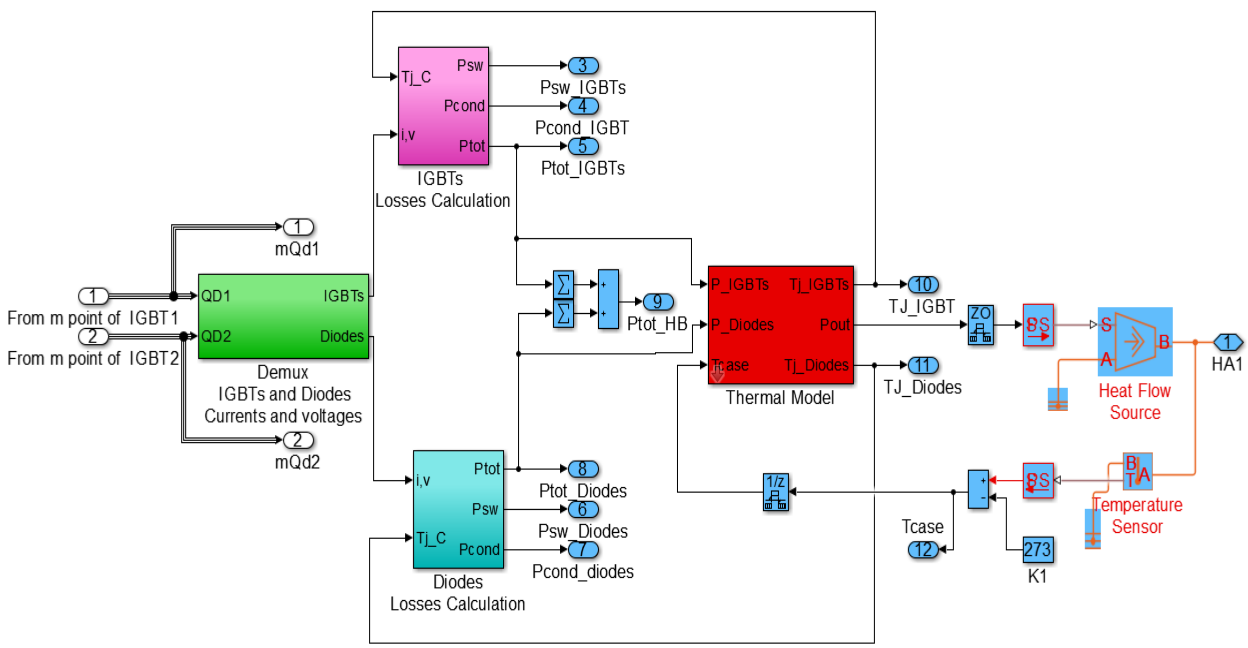

Figure 31: IGBT and Diode losses calculation model overview [31]

4.3.2 Masking of IGBT, Diode datasheet and initial conditions

The masking feature of MATLAB provides the benefits of saving input data in the Simulink model and when it is necessary to use the data then these data can be recalled from the particular masked block. For this simulation this feature is used to save the IGBT, diode characteristics curves and initial conditions.

The losses depend upon the characteristics of IGBT and diodes. Different components will show different losses at different temperature. The selection of IGBT and diodes depends upon the voltage, current and power requirements of applications. After selecting the devices to be used the characteristics curves (Switching on losses, E_{ON} Vs I_c; Switching off losses, E_{OFF} Vs I_c and I_c vs V_{CE} (all datasheet [32]shown in Figure 33) are loaded on the loss calculation block shown in Figure 31.On the other hand this task is done for the diodes(E_{rec} Vs I_f and I_f Vs V_f) also.(shown in Figure 34).Where,E_{rec}=reverse recovery energy, I_f=diode forward current,V_f=diode forward voltage.In order to run the simulation some parameters (mentioned in Table 6) are also considered as initial conditions and are also masked in the loss calculation block like IGBT and diodes.It is worth mentioning here that interpolation and extrapolation methods were used to find the values of losses in the range of the curves plotted in Figure 33 and Figure 34.

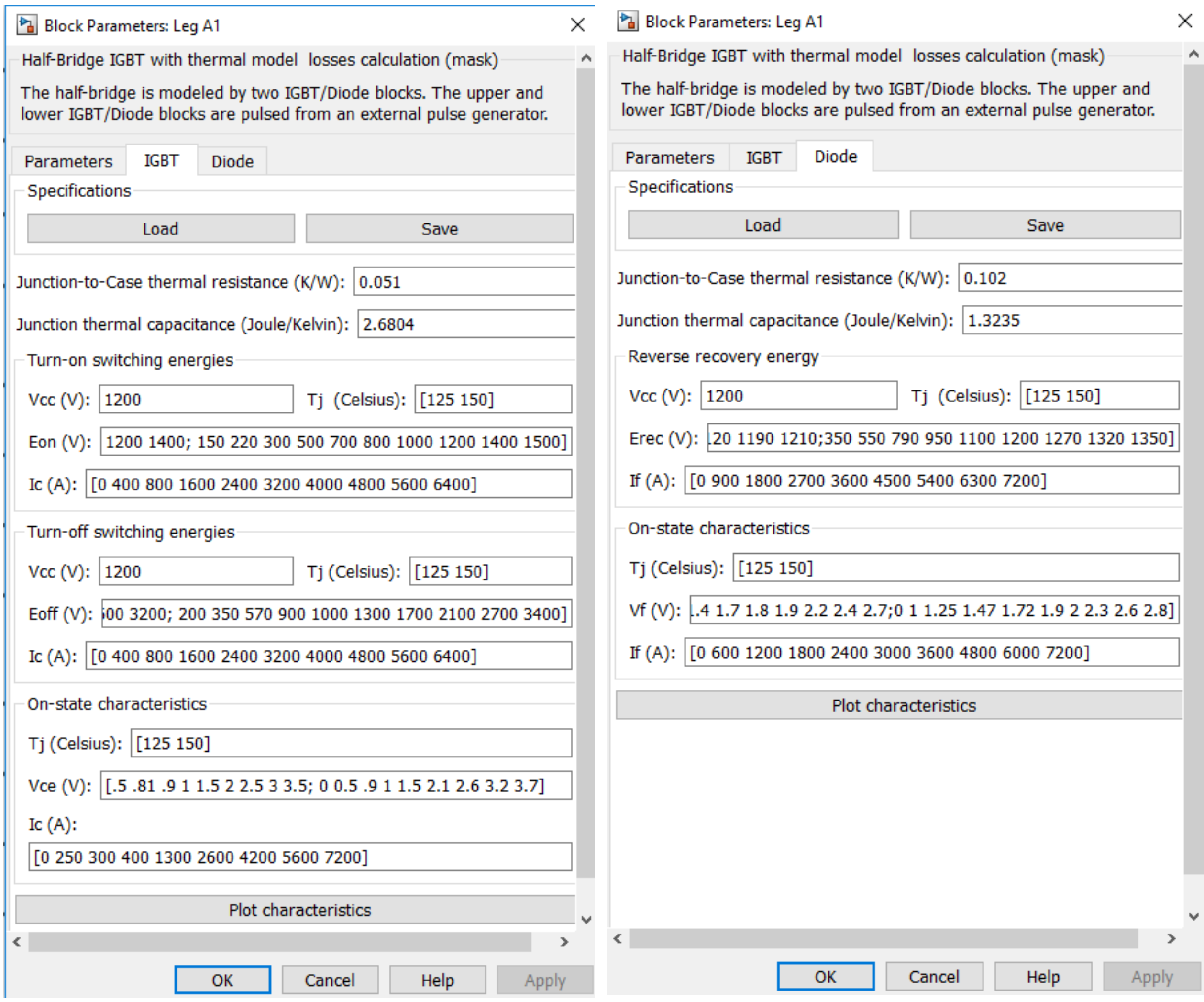

Figure 32: Masking of IGBT and Diode parameters [31]

Table 6: Initial condition masking parameters [31]

Parameter Name	Value
nternal resistance Ron (Ohms):	1,00E-03
Snubber resistance (Ohms):	1,00E+06
Initial Junction Temperature (degrees Celsius):	123
Pulse Duration for Energy-to-Power conversion (s):	z=.003;
Simscape Power Systems Sample Time (as specified in the Powergui) (s):	5,00E+09
Simscape Solver Sample Time (s):	5,00E+10

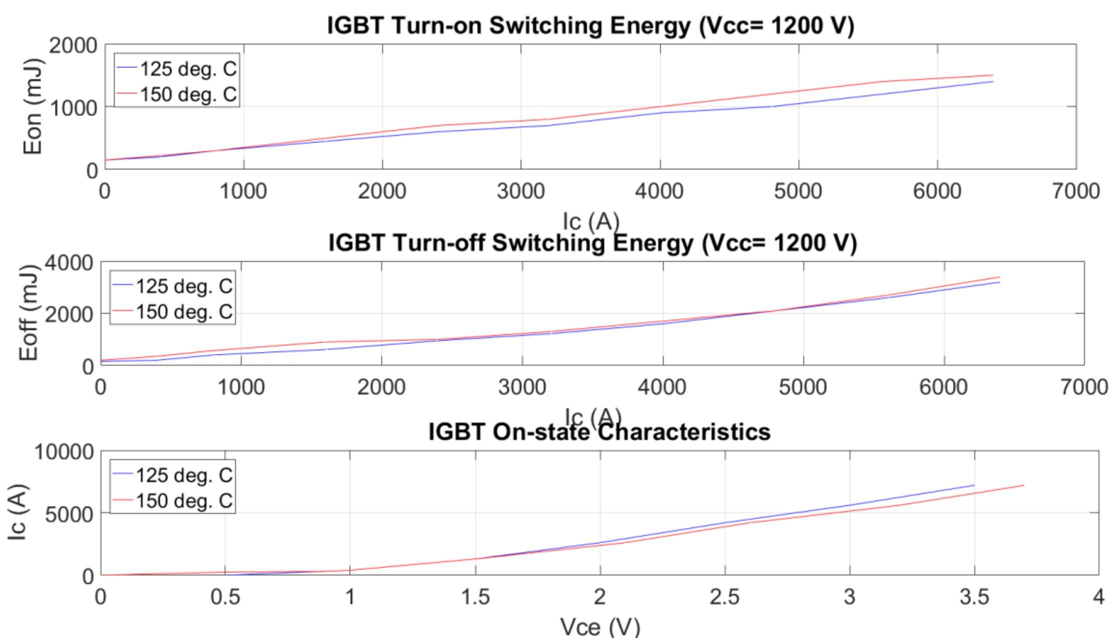

Figure 33: IGBT characteristics curves [32]

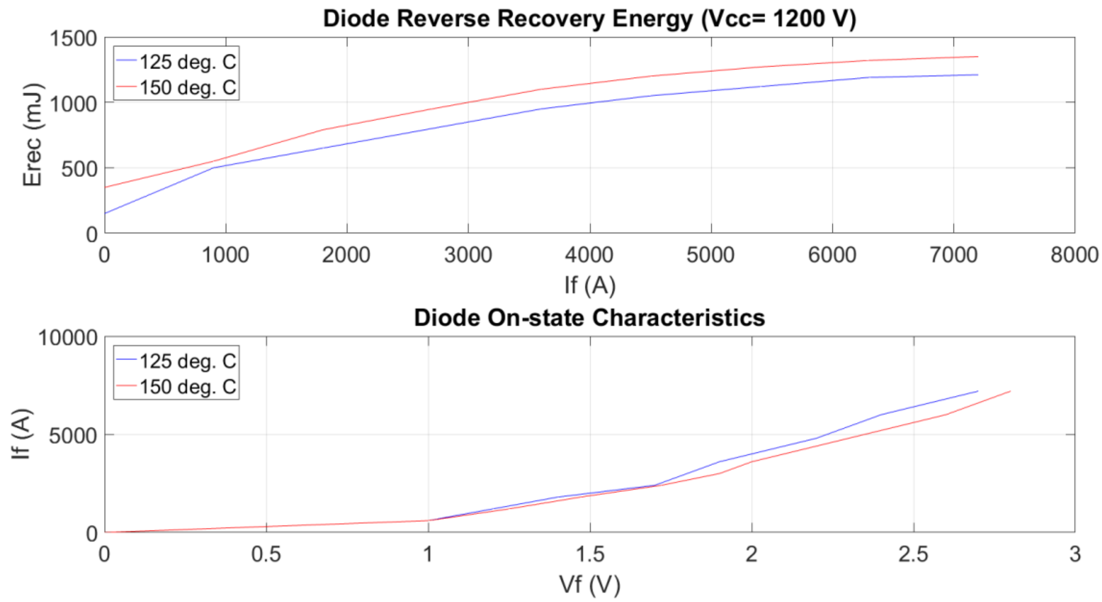

Figure 34: Diode characteristics curves [32]

In the next sections the block diagrams of Figure 31 will be explained in details.

4.3.3 ,, Demultiplexing of IGBTs,diodes currents and voltages'' block

From the m point of IGBT 1(denoted by QD1 in Figure 35) and IGBT 2(QD2 in Figure 35) the information of the flowing current (found during switching on state) and the voltage across them (found during switching off state) are given input to this block (shown in Figure 31).After that the current through the diode and IGBT is separated (denoted by I_Q and I_D; top and bottom for IGBT 1 and IGBT 2 respectively), so as the voltages. The demuliplexed current and voltage of IGBT 1,IGBT 2(shown inFigure 36) and diode 1,diode 2 are shown below(inFigure 37).

After separating individual voltages and currents of IGBTs and diodes, these data are sent to ,,**IGBT loss calculation''** and ,,**Diode loss calculation''** blocks(shown in Figure 31).

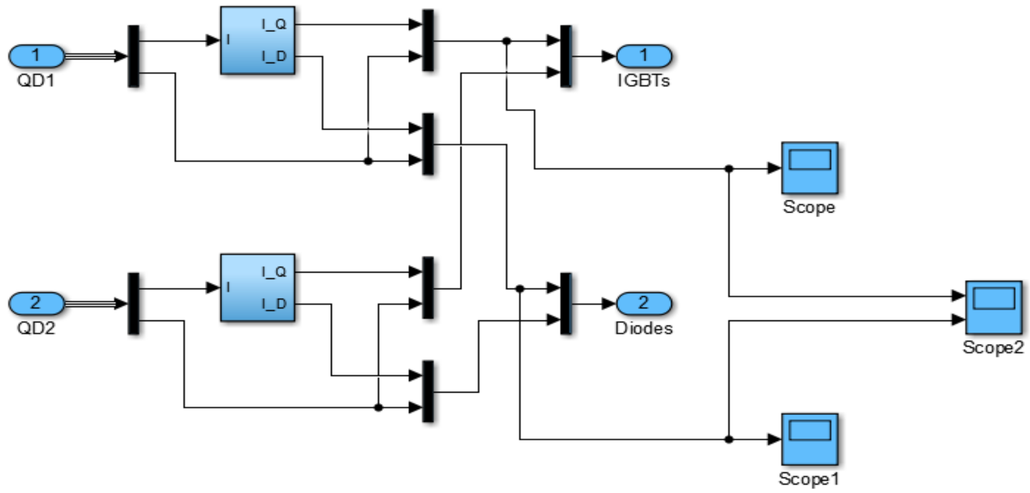

Figure 35: Demultiplexing connection of Currents and voltages of IGBT 1(QD1) [31]

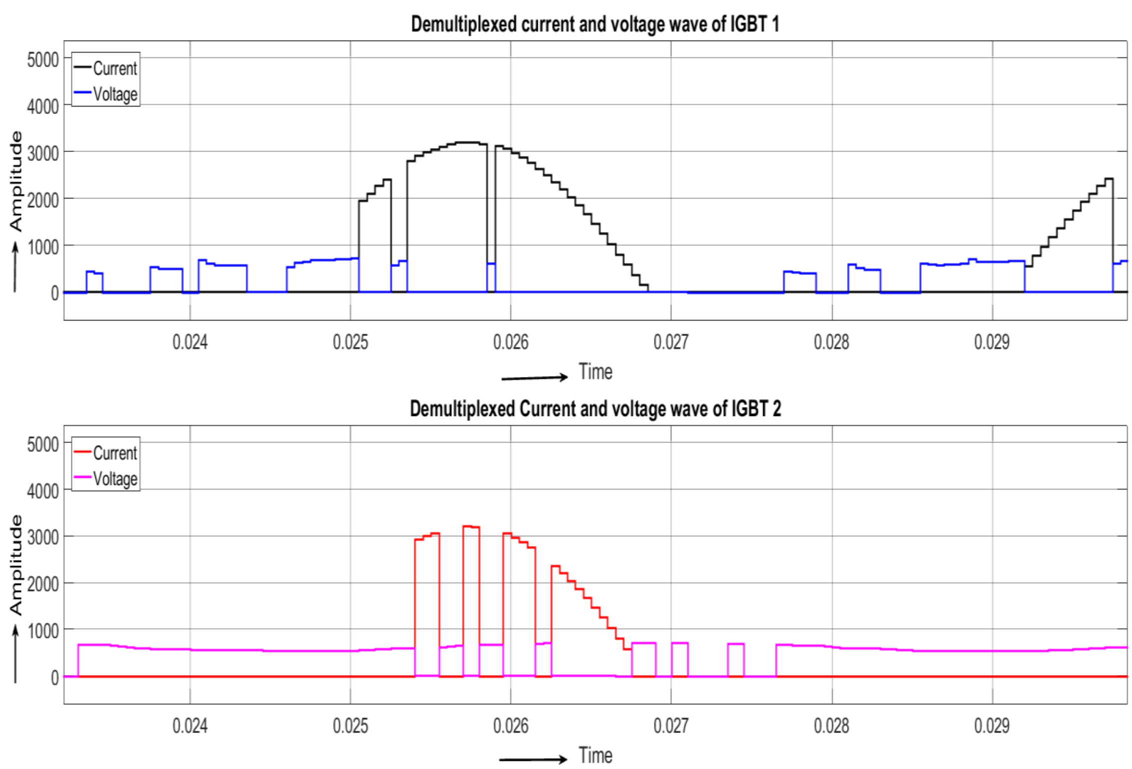

Figure 36: Demultiplexed output of IGBTs

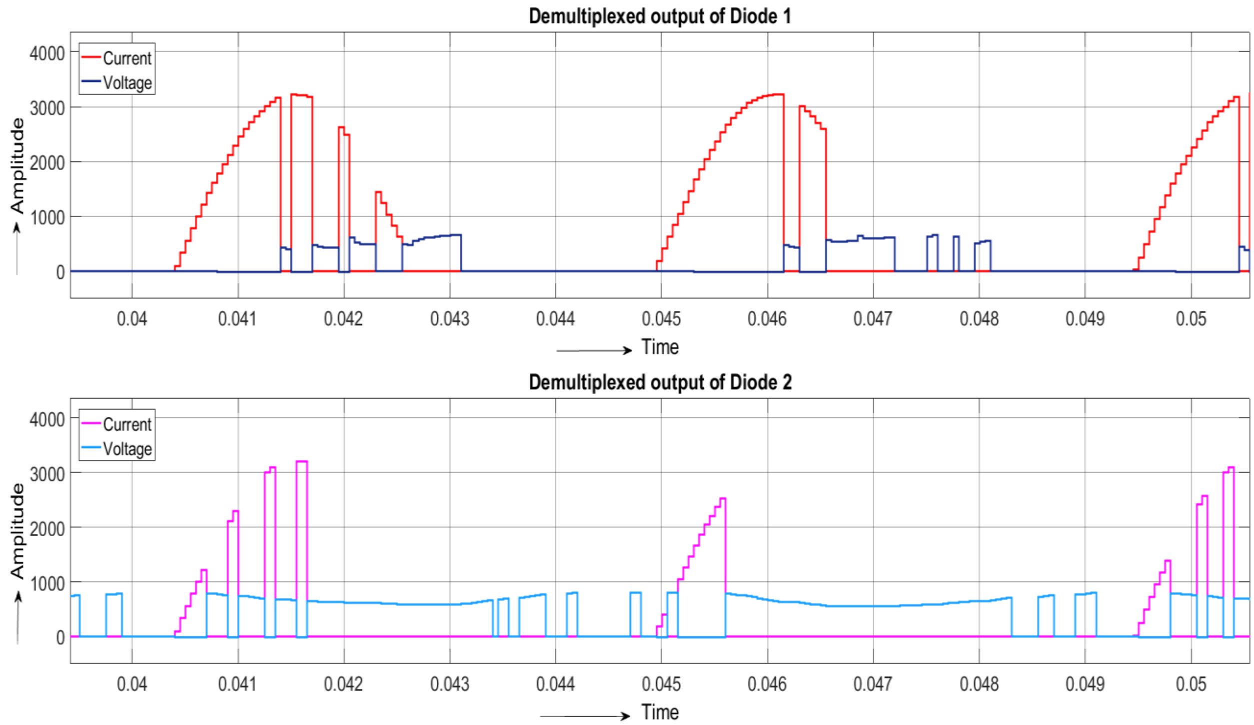

Figure 37: Demultiplexed output of diodes vs time(in seconds)

4.3.4 ,, IGBTs Losses Calculation'' block

Based on the data found on the previous block and with the masked parameters (in section 4.3.2 Masking of IGBT, Diode datasheet and initial conditions) the losses are calculated. The loss calculation block consists of three table data :(masked with the block) switching on (marked yellow color in Figure 39), switching off (marked red color in Figure 36) and conduction loss (marked green color Figure 36).

At first the currents and voltages are separated by the selector block (Figure 36).Based on the current flowing the decision of switching on and off is made and depending on that the switching on and off triggering pulses are generated, given to the switching on (colored magenta in (Figure 36)and off (colored orange in (Figure 37) blocks respectively.

Before inputting a voltage value in the switching on and switching off losses a memory block is used in either case. It means if the voltage connection is inputted directly on the switching on block then while connecting it the switching off block a memory block is used there. The logic is if the switching on block is getting a present status value then the switching off block must hold the previous state value. If a memory block is not used then then two blocks would show the same curve of losses.

Switching on and off losses are functions of temperature, voltage and currents. These three parameters are given as input in the two look up tables (colored yellow and red respectively for switching on and switching off).

In the 3rd block (bottom, green block of Figure 38) take the information of current and temperature to calculate the conduction losses.

After calculating the losses the data is sent to the thermal model block (In Figure 31) for temperature rise calculation.

The losses occurred in a particular IGBT of phase A is shown below in Figure 39.It can be summarized from the losses graph that the conduction losses are much greater than the switching losses. On the other hand the switching off losses is smaller than the switching on losses.

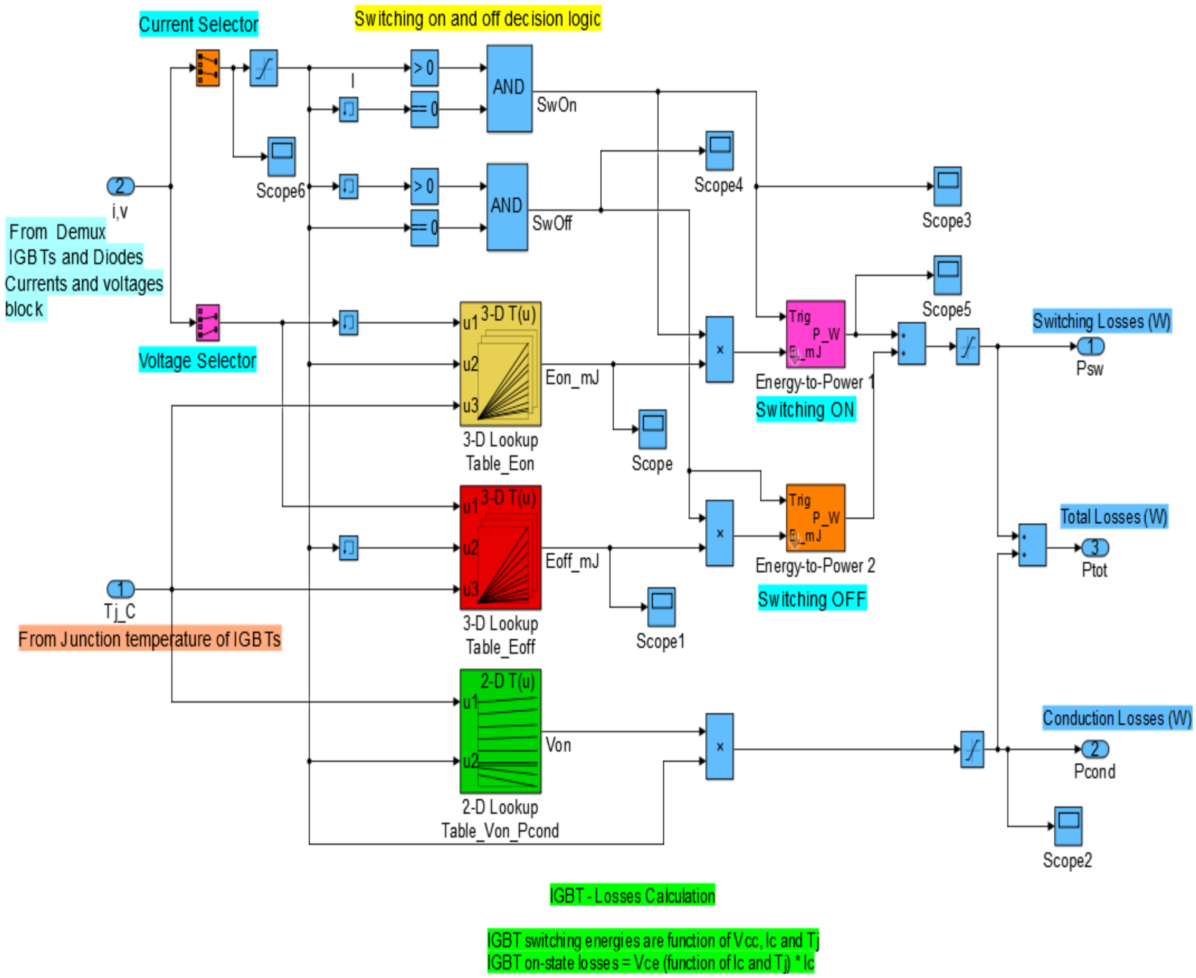

Figure 38: IGBT Losses calculation block internal architecture [31]

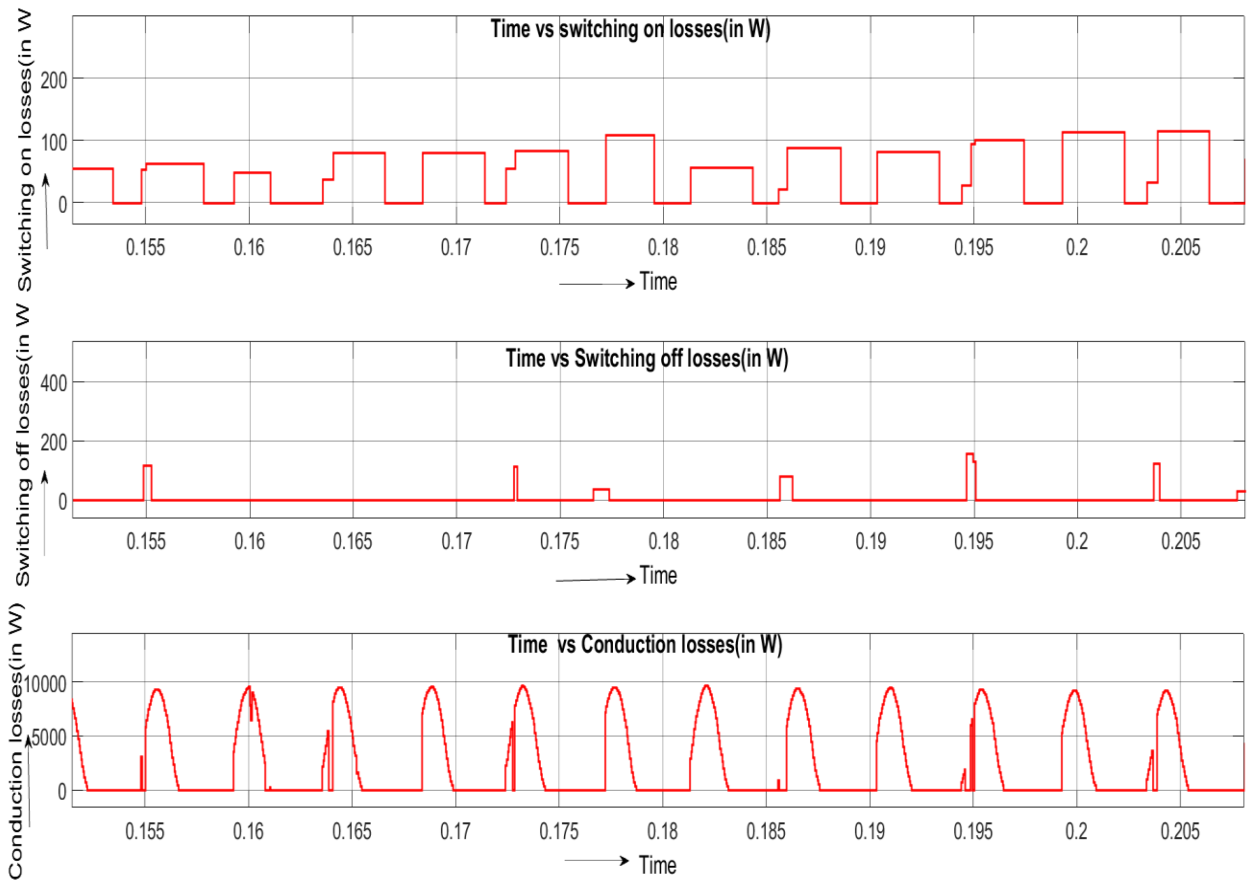

Figure 39: IGBT Losses graph for switching on, switching off and conduction losses vs Time

4.3.5,, Diode Losses Calculation'' block

Generally, two types of losses are found in a diode. Reverse recovery losses and conduction losses. When the diode conducts from a forward conduction phase to a reverse conduction phase then it is referred to as reverse recovery losses. [33]

In order to calculate the diode losses the data from the demux block of currents and voltages are taken. The current information is used to create the triggering pulses for the reverse recovery current losses of diodes (mentioned as switching on and off logic in Figure 40).

There are needed three parameters to calculate the reverse recovery losses (current, voltage and temperature).These current and voltage data are taken from the demultiplexing block while the temperature data is inputted from the junction temperature of diodes.

The diode reverse recovery losses and conduction losses are plotted in Figure 41.It can be shown in the Figure 41 that the reverse recovery losses are much smaller than the conduction losses.

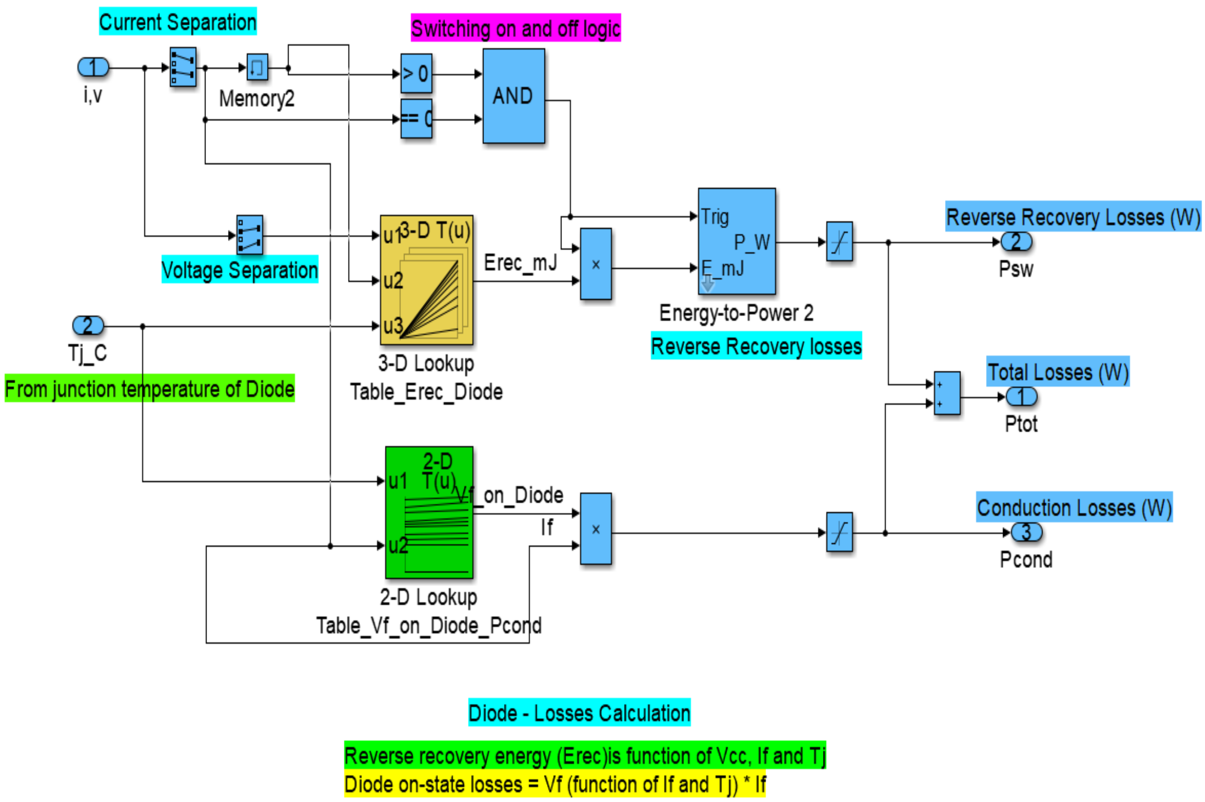

Figure 40: Diode Losses calculation block internal architecture [31]

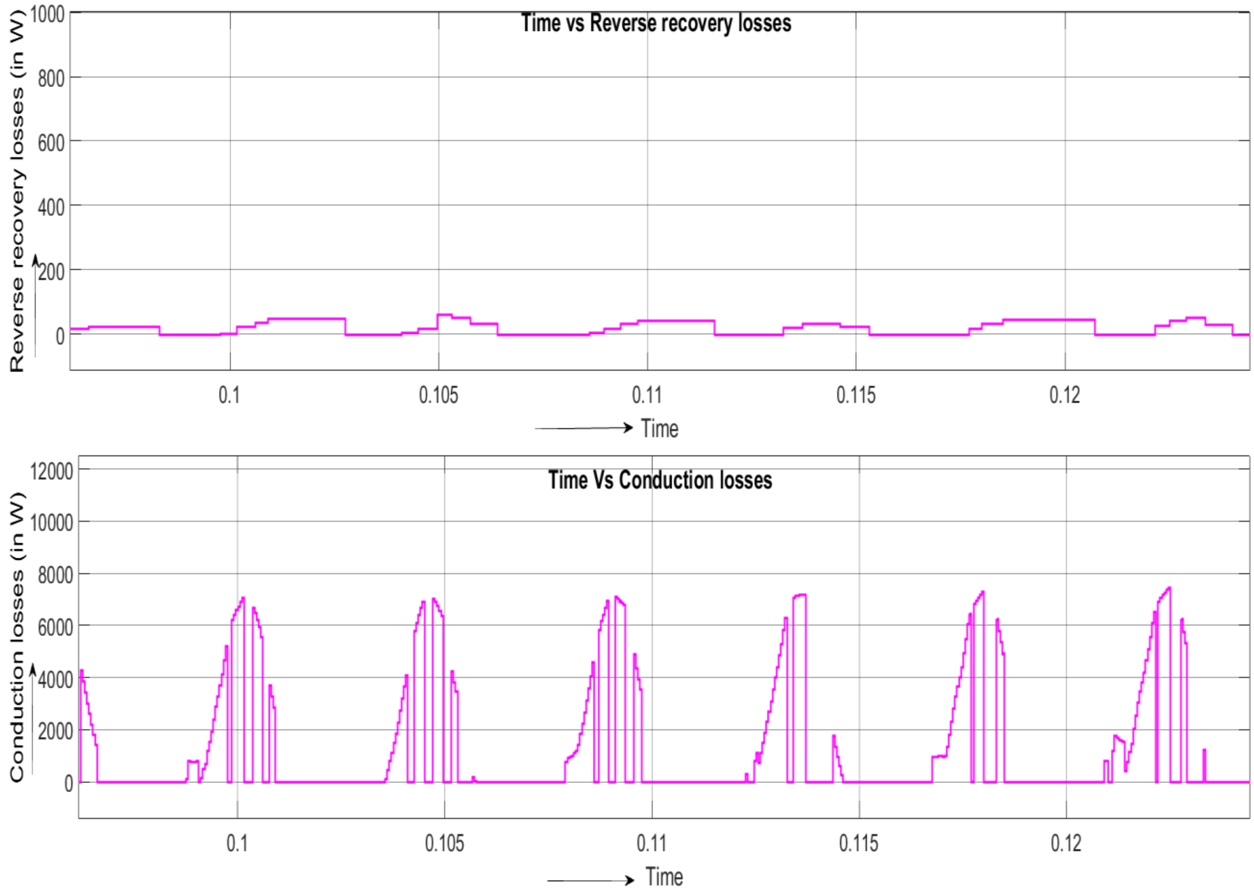

Figure 41: Diode Losses graph for reverse recovery and conduction losses vs time (in seconds)

4.3.6 ,, Thermal model '' block

The thermal model block converts the generated power to temperature rise in the IGBT and diodes. Here, the state space model has been utilized to calculate the temperature rise. The value of A,B,C,D parameters are calculated in the masked system.

The memory block after the state space model before taking the output is used to create a time delay since the rising of heat transfer takes some time to exchange the heat. The raised temperature curve in the IGBT and diode is shown below in Figure 43 .The simulation was run till 2s and it is observed that the temperature raised up to 700°C. This temperature rise is calculated according to the heat sink and thermal resistance of the devices used here. But in practical case by using different materials of different thermal resistance, thermal masses the temperature rise can be controlled which is out of scope of this work. For this work only it is shown that the temperature rise can be calculated by using this model.

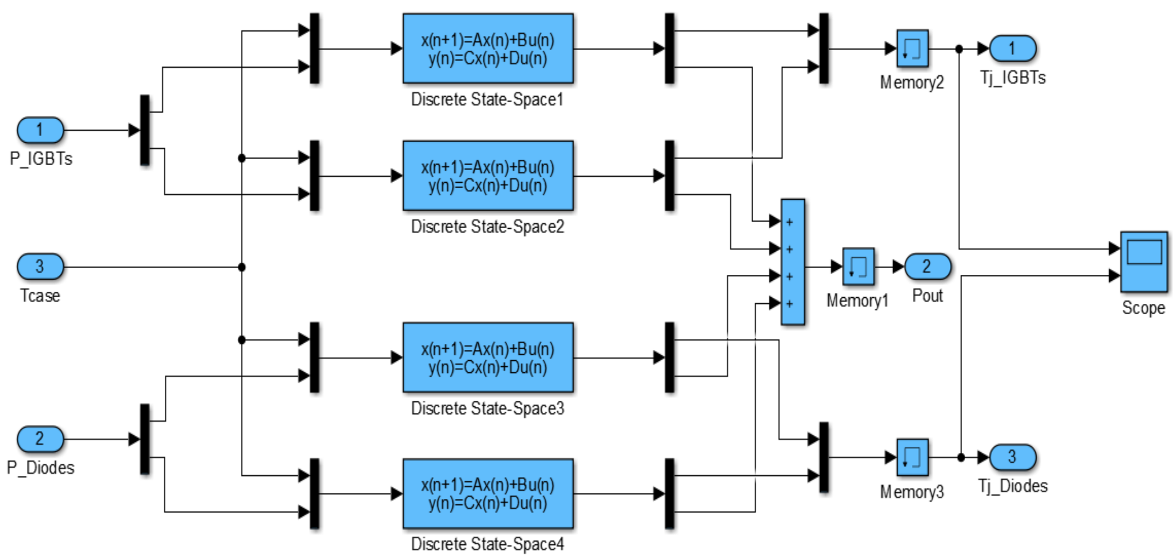

Figure 42: Thermal model internal architecture [31]

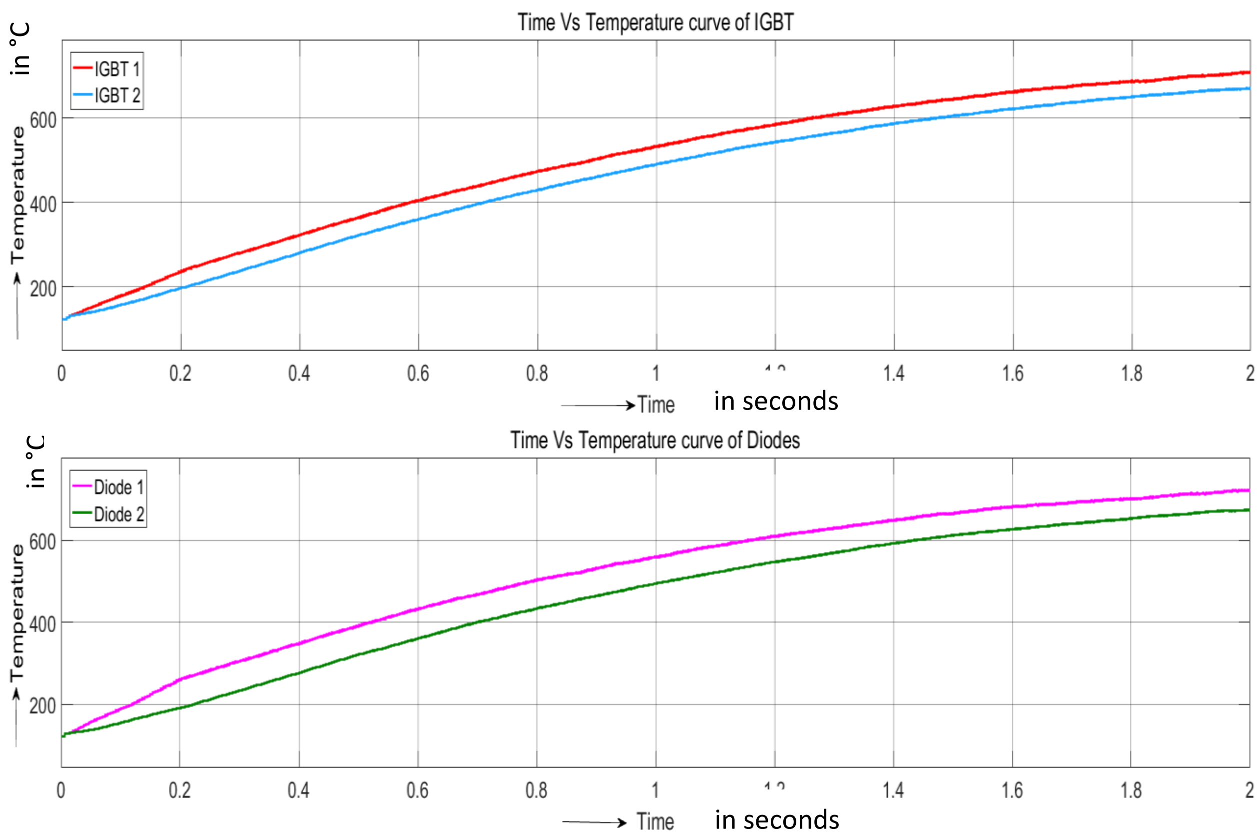

Figure 43: Time vs temperature curve of IGBT and diode

4.4 Total loss Curves of IGBTs and Diodes and efficiency

In this section the overall losses occurred in each phases and overall efficiency have been discussed. There are four IGBT switches, four freewheeling diodes in parallel with IGBT in each phase. In total there are 16 IGBTs and 16 diodes are in the three phase system.

In Figure 44 and Figure 45 phase A's all IGBT and diode losses are plotted. In Figure 46, Figure 47 phase B losses and Phase C has been plotted in Figure 48,Figure 49

The total losses occurred in Phase A,Phase B,Phase C are plotted in Figure 50.

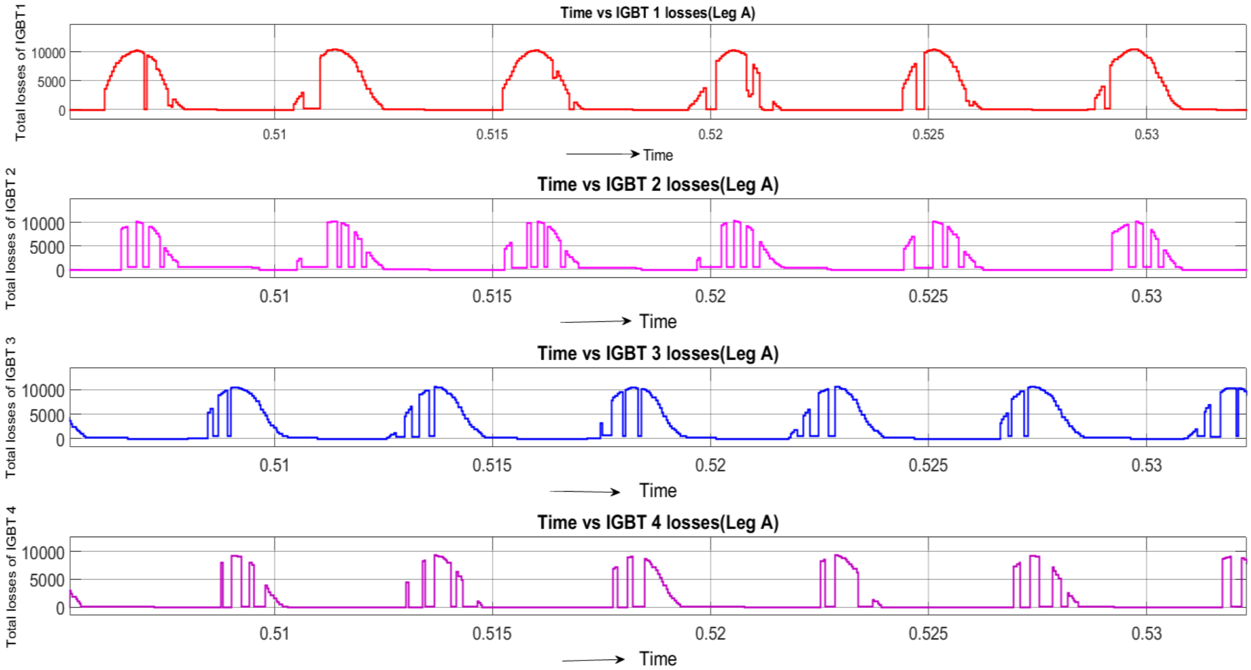

Figure 44: Phase A all IGBT losses (in W) vs time (in seconds)

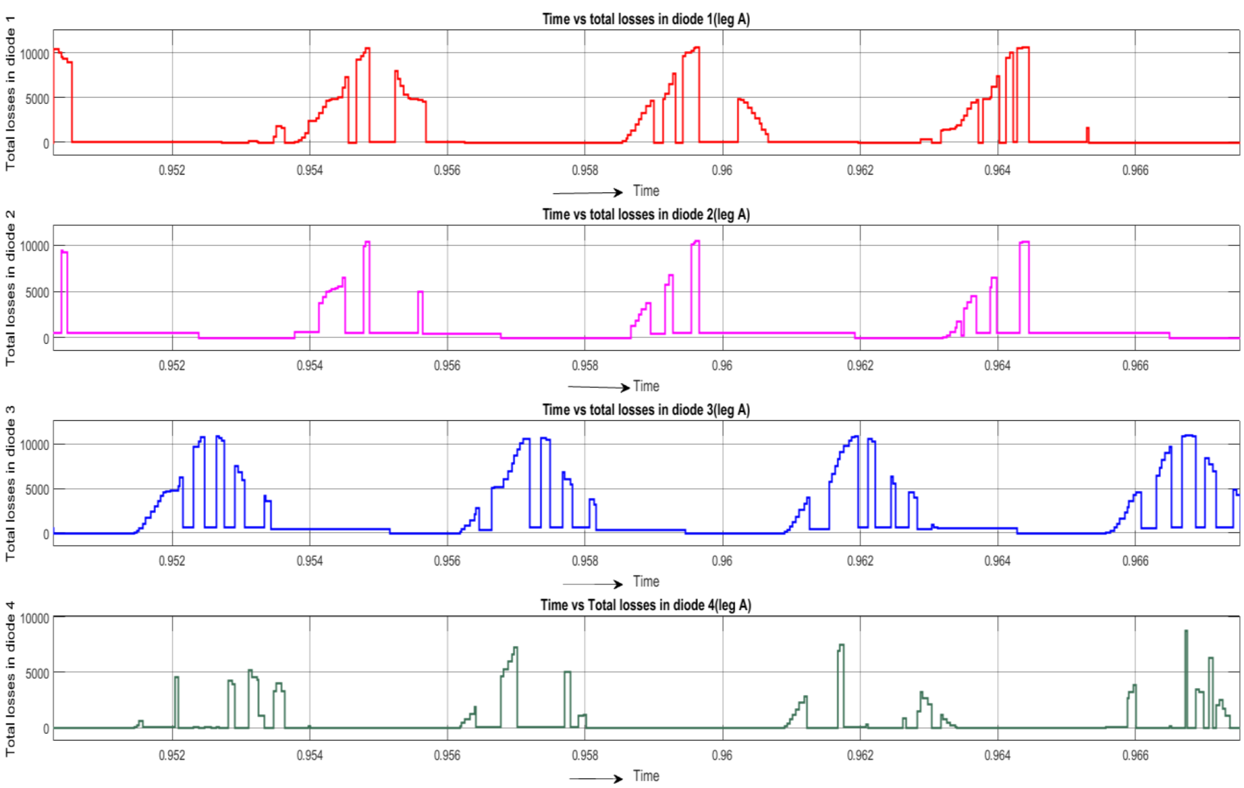

Figure 45: Phase A all Diode losses (in W) vs time (in seconds)

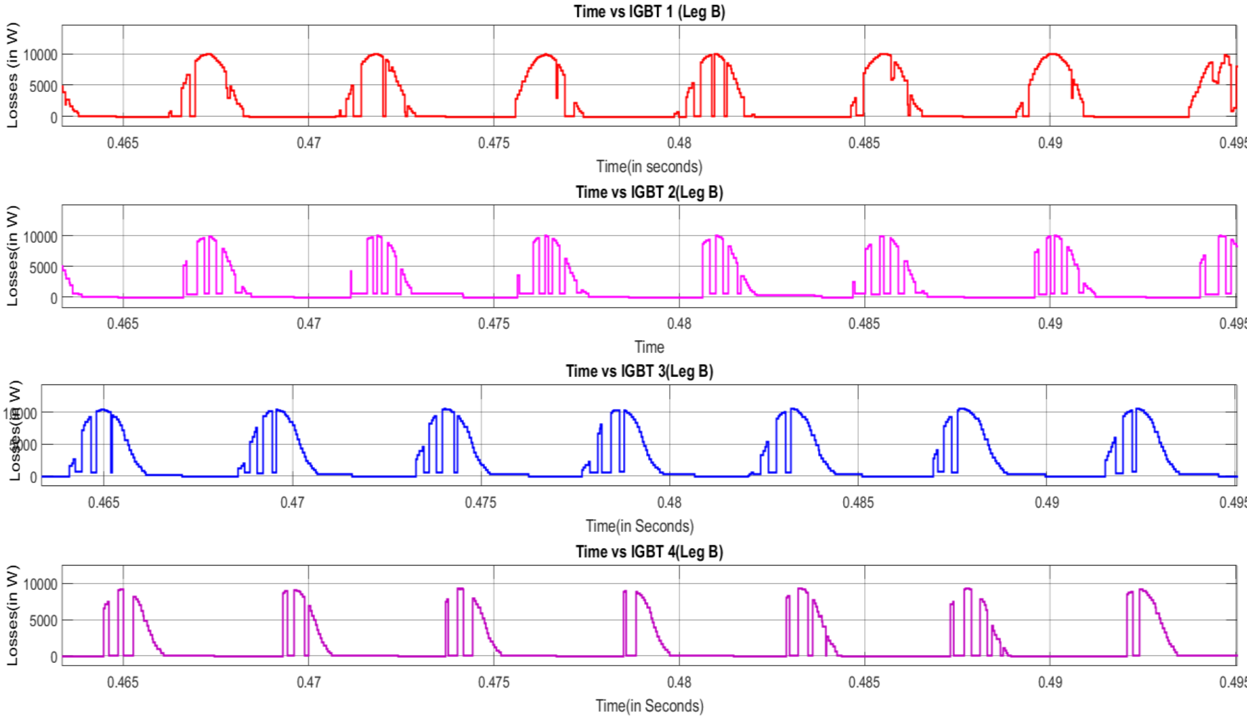

Figure 46:Phase B all IGBT losses

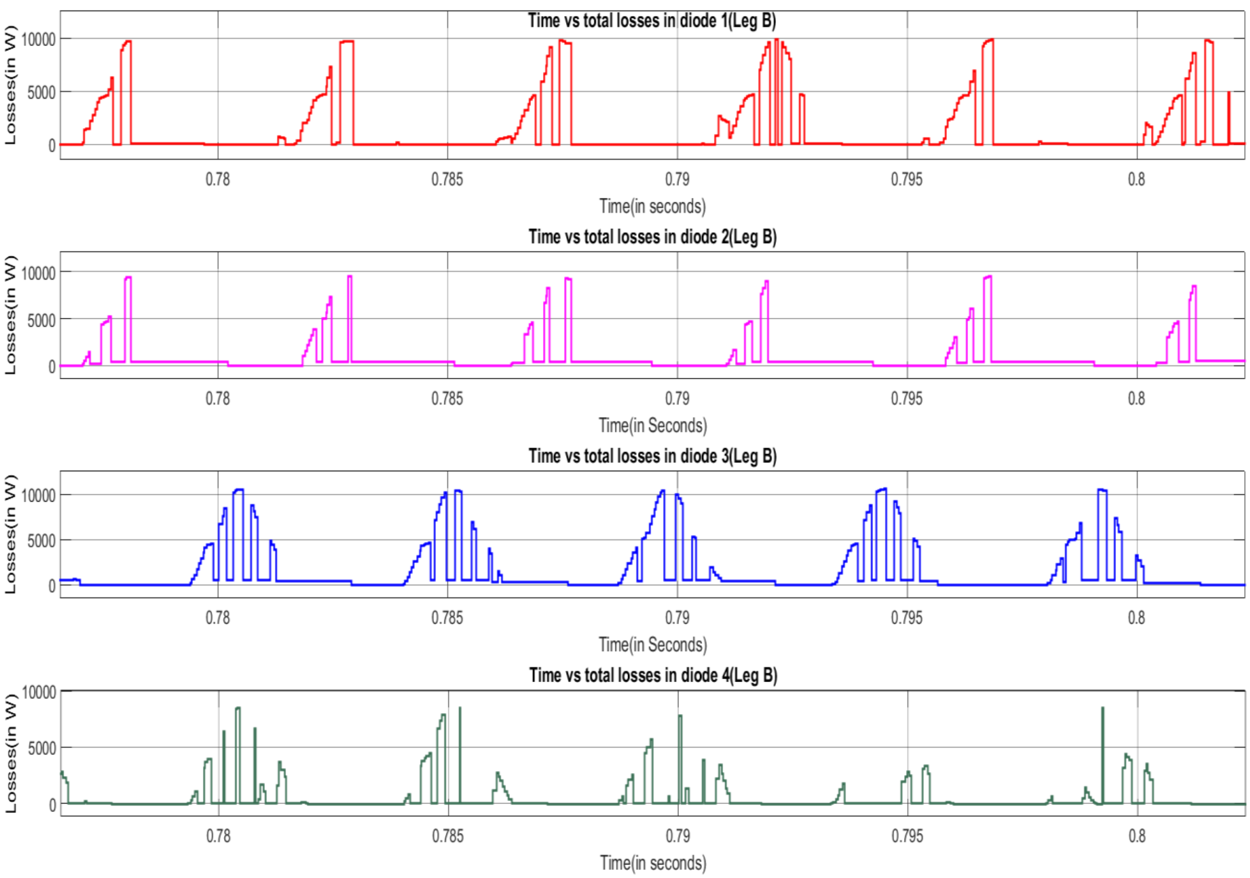

Figure 47:Phase B all diode losses vs time

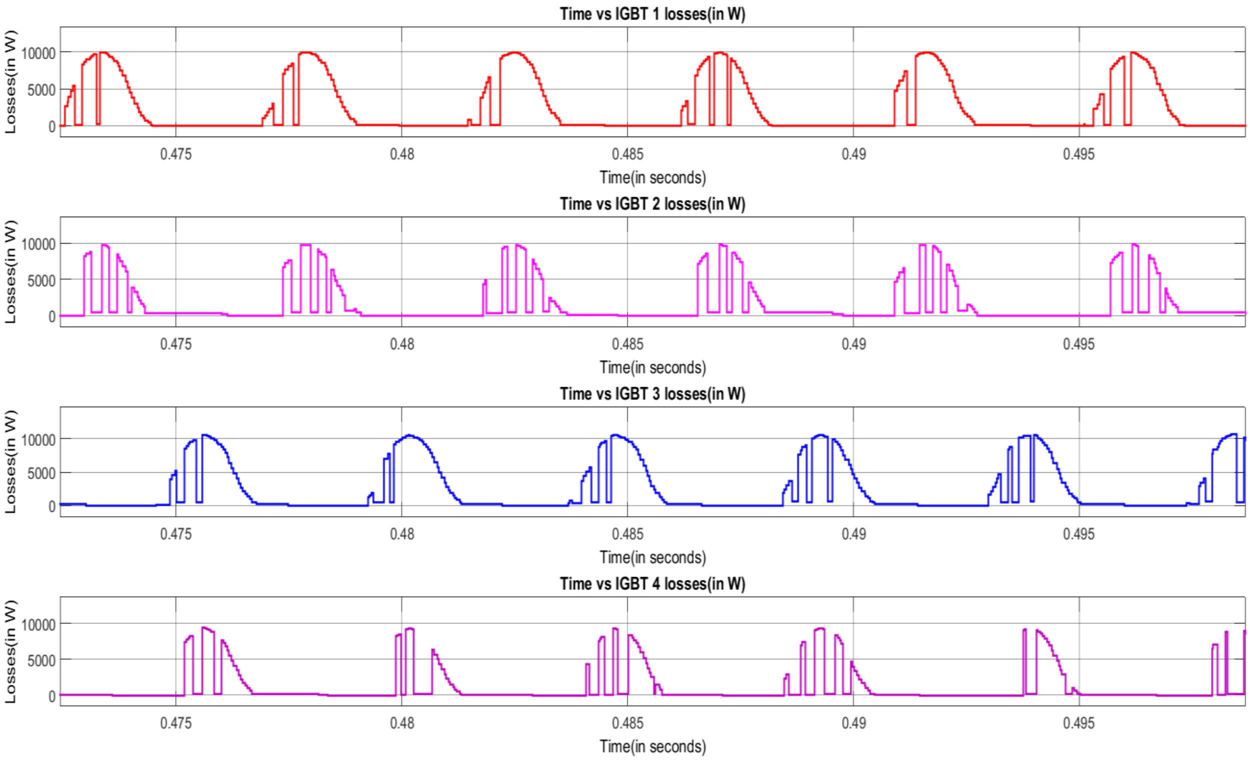

Figure 48.Phase C all IGBT losses vs time

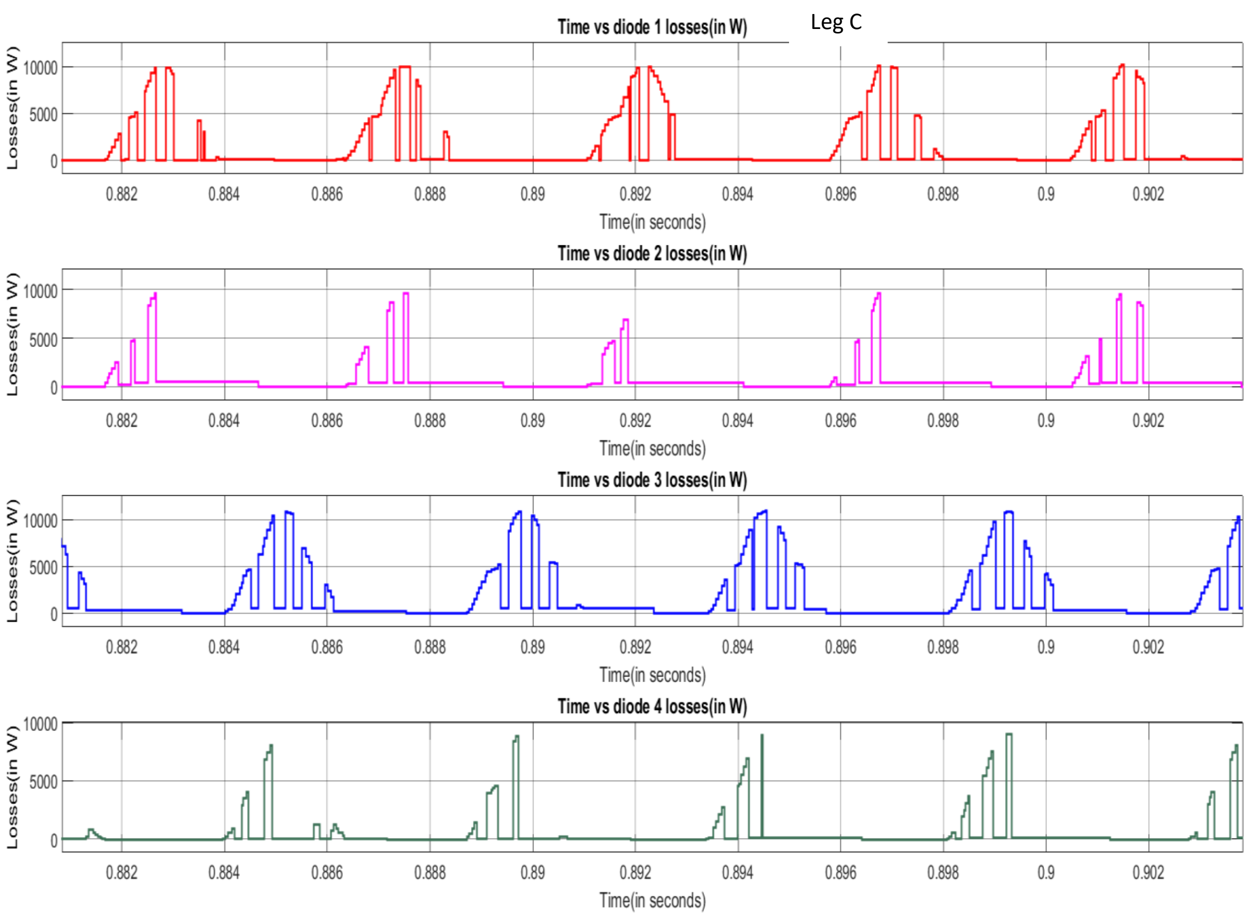

Figure 49: Phase C all diode losses vs time

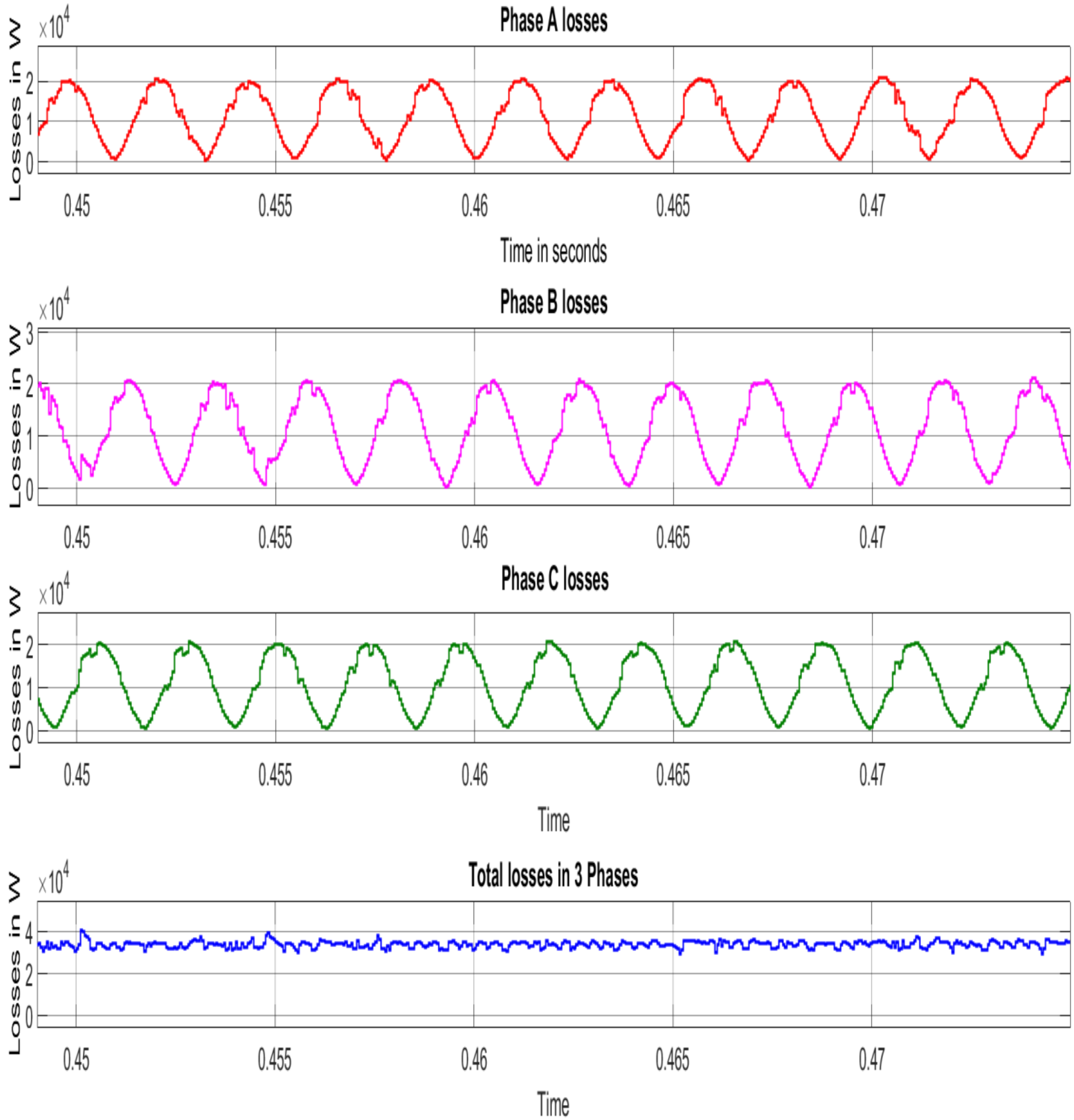

Figure 50:Phase A,B,C losses and total losses(bottom) vs time

The instantaneous efficiency curve is shown below. In order to calculate the instantaneous efficiency the instantaneous losses and power are taken. The efficiency has been expressed in percentage.

Figure 51: Instantaneous efficiency curve

4.5 Thermal model of inverter system

The IGBT and the diode cause power losses from the conduction and switching characteristics. This power generates heat in their surfaces. Through conduction heat is transferred to the case. The case is attached with the heat sink. From heat sink heat is dissipated in the environment. The conduction of heat is represented by some equivalent thermal resistances from IGBT or Diode to Case(Zth_JC_Q),Case to heat sink(Zth_CH) and after that heat sink to environment(Zth_HA) which is represented in the Figure 52.

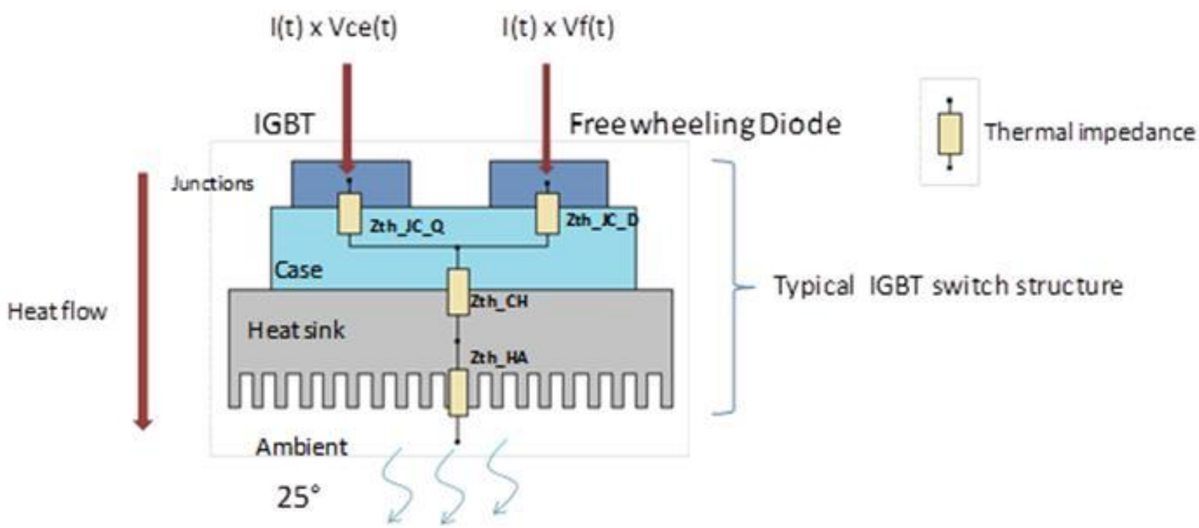

Figure 52: Thermal model of inverter system [34]

4.5.1 Simulink block diagram to calculate the thermal system

The power losses of IGBT and diode are given as input to the Thermal model block(referred to Figure 31).In this block the state space model of the generalized equation $P=\Delta t*Zth_{JC\_Q}$ is used to calculate the temperature of the IGBT junctions. For diode the same equation is applied but in this case the equivalent thermal impedance used is Zth_{-JC_D}.

When the heat is calculated in the IGBT surfaces then it is transported to the case (shown in Figure 53) and the block of Figure 52left side) represents the ,,case''. An equivalent heat source thermal mass is considered here to approximate the ,,case''.,, The ,,Case'' block represents a thermal mass, which is the ability of a material or combination of materials to store internal energy. The property is characterized by mass of the material and its specific heat.'' [35]

The generated heat is then transferred to the heat sink. Between them the heat flow cannot flow smoothly to the heat sink which is approximated by an equivalent thermal impedance block immediately after case 1 block.

Similarly, this process of approximation is done for heatsink to environment heat dissipation. Heat sink mass has been considered according to the material properties that is going to be used for heat sink and the impedance value between heat sink and environment is chosen according to the heat flow capability of the heat sink to dissipate heat in the environment(shown in Figure 53).

The temperature source is used to approximate the dissipation of heat to the environment., The block represents an ideal source of thermal energy that is powerful enough to maintain specified temperature at its outlet regardless of the heat flow consumed by the system'' [35]

In order to visualize the rising temperature in different locations (case, heat sink), a temperature sensor is used to measure the temperatures.

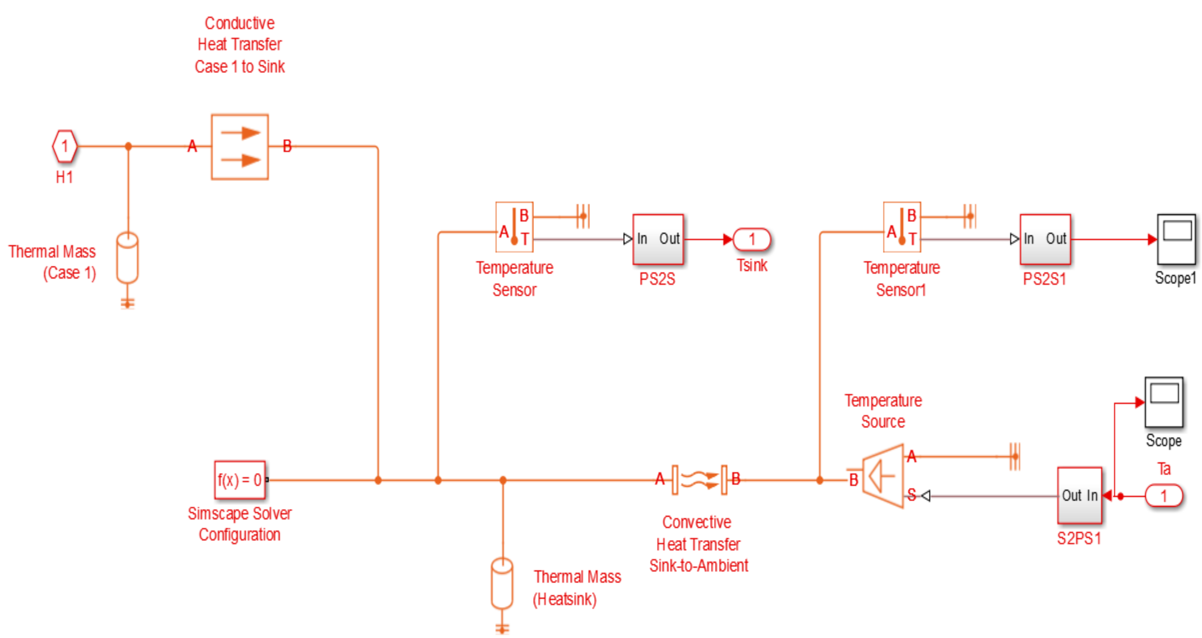

Figure 53: Thermal model Simulink block [31]

4.5.2 Simulation results of thermal system

In this section the temperature rise curves in the case, heat sink is shown. To simulate the system some approximate data are taken mentioned in Table 7 below.

Table 7: Impedance values of different sections in the thermal system [31]

Parameters	Value
$IGBT_{RTH-JC}$	.051 K/KW
$IGBT_{CTH-JC}$	2.6804 J/K
$Diode_{RTH-JC}$	.102 K/KW
$Diode_{CTH-JC}$	1.3235 J/K

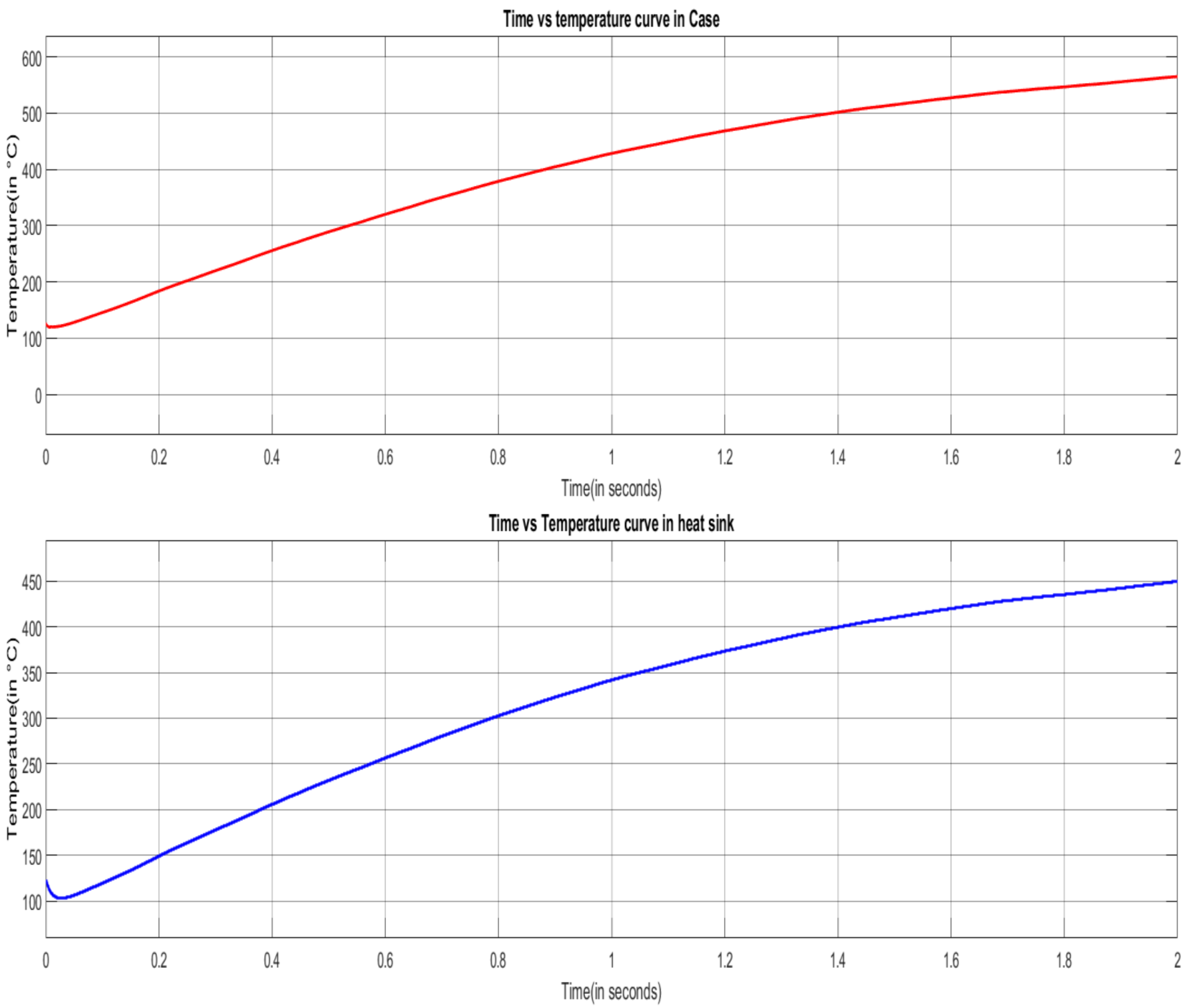

Figure 54: Time vs case temperature (top) and heat sink temperature (bottom) curve

5. Outlook

In this task only the phase disposition modulation technique for the 3 level converter has been shown. The effect of other PWM techniques like phase opposition disposition, alternate phase opposition disposition, space vector modulation techniques could be researched. Which might improve the harmonics in the phase voltages.

The corresponding losses, raised temperature in the IGBT, diodes, heat sinks has been observed and checked whether they fit with the model or not. But they were not designed in the optimum level. The cooling system can be realized, designed and tested by using the designed loss model here.

The whole model consists of the wind turbine and the generator only. But the grid side converter has not been integrated and the grid connection also not done here. Which could be connected with this model. The loss model which has been built here could also be used to find the losses in the grid side converter.

6. Conclusion

Finally, the main tasks which have been done in this prethesis were a suitable 3 level FC converter design for the machine side and the corresponding losses calculation of the converter. In addition to the previous task the thermal model also realized which shows the temperature status in the IGBTs, diodes, junctions, heat sinks and in the end the efficiency curve is presented to show the overall performance of the designed converter. The efficiency found was approximately 98.5%.

7. References

[1] J. Svensson, "Grid-connected Voltage Source Converter," Göteborg,Sweden, 1998.

[2] M. R. I. G. G. Z. Zhu, "Power converters for wind turbines: Current and future development," August 2013.

[3] M. M. A. B. Sajid Hussain Qazi, "Simulation of PMSG based Wind Energy system with Multi Level NPC Converter," *4th International Multi-Topic Conference,* February 2015.

[4] F. &. C. Z. Deng, "Low-voltage ride-through of variable speed wind turbines with permanent magnet synchronous generator," in *10.1109/IECON.2009.5414992. IECON Proceedings (Industrial Electronics Conference)*, 2009.

[5] [Online]. Available: http://www.wind-power-program.com/turbine_characteristics.htm. [Accessed 19 02 2019].

[6] [Online]. Available: https://en.wikipedia.org/wiki/Yaw-rate_sensor. [Accessed 04 02 2019].

[7] [Online]. Available: https://www.windpowerengineering.com/mechanical/brakes/brakes-101/ . [Accessed 04 02 2019].

[8] M. Aarya.A1, "Multilevel Inverters-A Comparative Analysis," *IOSR Journal of Electrical and Electronics Engineering (IOSR-JEEE) ,* pp. e-ISSN: 2278-1676,p-ISSN: 2320-3331,.

[9] M. H. Rashid, -“Power Electronics-Circuits, Devices and Applications” Pearson Education Incorporated, 2005.

[10] I. Ouerdani, A. B.-B. Abdelghani, I. Slama-Belkhodja and D. Montcsinos-Miracle, "Three-level flying capacitor converter control for DC smart grid connection," in *IEEE*, Sousse, Tunisia, 24-26 March 2015.

[11] B. R. a. M. M. Simple Analysis of a Flying Capacitor A.Ruderman(1), "Simple Analysis of a Flying Capacitor Converter Voltage Balance Dynamics for DC Modulation," *13th International Power Electronics and Motion Control Conference (EPE-PEMC 2008),* pp. 260-267, 2008.

[12] M. A. M. N. &. S. N. Mohd Esa1, "Harmonic Analysis of Three level Flying Capacitor Inverter," *International Research Journal of Engineering and Technology (IRJET),* p. Volume: 04 Issue: 10, Oct - 2017 .

[13] "Flying capacitor mulitlevel inverter," [Online]. Available: http://engineering.electricalequipment.org/electrical distribution/ flyingcapacitormultilevelinverters.html. [Accessed 16 02 2019].

[14] A. a. G. A. K. a. G. A. a. J. A. Shukla, "A Three-level Flying Capacitor Inverter for SSSC Applications," *IEEE Power Engineering Society General Meeting,* pp. pp. 1453-1458 Vol.2., 10 January 2005.

[15] U. a. R. E. W. P. Ned Mohan, Power Electronics,Converters,Applications and design.

[16] K. P. P.S.Bimbhra, Power Electronics.

[17] P. d. i. J. M. ir. Steven Thielemans, "Balancing mechanisms for flying capacitors MLI," January 2008.

[18] S. G. M. M. R. S. G. S. G. Carrara, "A New Multilevel PWM Method: A Theoretical Analysis," *IEEE Transactions on Power Electronics,* Vols. Vol. 7, No. 3, 1992.

[19] T. A. L. D. G. Holmes, "Pulse Width Modulation for Power Converters: Principles and Practice," *IEEE Press, J. Wiley & Sons,* 2003.

[20] S.J Watkins and L. Zhang, "Influence of multilevel sinusoidal PWM schemes on the performance of a flying capacitor inverter,," *S.J Watkins and L. Zhang,’’Influence of multilevel sinusoidal PWM schemeInt. Conf Power Electronics, Machines and Drives ,* pp. pp. 92-97, 2002.

[21] T. Colella, "Engineering Manager,electrocube".*How to Select a DC link capacitor.*

[22] W.-S. &. T. Y.-Y. Chien, " Analysis and design on the reduction of DC-link electrolytic capacitor for AC/DC/AC converter applied to AC motor drives," pp. 275 - 279 vol.1. 10.1109/PESC.1998.701911., ..

[23] Y.-K. W.-J. L.-J. L. Shih-Yu Yang, "Integrated mechanical and electrical non-salient pole PMSG-based wind turbine," in *IEEE*, Addison, TX, USA, 18-22 Oct. 2015.

[24] Chaturvedi, Pradyumn & Jain, Shailendra & Agrawal, Pramod & Nema, Rajesh & K. Sao, Kaushal. (2008). Switching losses and harmonic investigations in multilevel inverters. IETE Journal of Research. 54. 10.4103/0377-2063.44233.

[25] 18 01 2019. [Online]. Available: https://www.electronics-tutorials.ws/rc/rc_1.html.

[26] C. B. a. C. Bull, "IGBT or MOSFET: Choose Wisely".*International Rectifier.*

[27] H. G. Eckel, *Topic Description, Semiconductor devices/Lecture Power Electronics, Rostock 2018,* Rostock 2018.

[28] M. P. D r . D u š an Graovac, "IGBT Power Losses Calculation Using the Data-Sheet Parameters," January 2009.

[29] K. GIANNOULOUDIS, "Power Losses and Thermal Impedance," Chalmers University of Technology, Gothenburg, Sweden.

[30] M. P. D r . D u š an Graovac, "IGBT Power Losses Calculation Using the Data-Sheet Parameters," January 2009.

[31] [Online]. Available: https://de.mathworks.com/help/physmod/sps/examples/loss-calculation-in-a-three-phase-3-level-inverter.html#d120e17564. [Accessed 17 12 2018].

[32] [Online]. Available: 16]https://www.infineon.com/dgdl/Infineon-FZ3600R17HP4-DS-v02_02-en_de.pdf?fileId=db3a30432313ff5e01235601c5db1610.

[33] [Online].Available: https://www.maximintegrated.com/en/glossary/definitions.mvp/term/Reverse%20Recovery%20Time/gpk/1015. [Accessed 12 02 2019].

[34] [Online]. Available: http://www.ni.com/white-paper/14743/en/. [Accessed 13 01 2019].

[35] [Online]. Available: www.mathworks.com.

8.Appendix

-Model

-References

-Further references

-Softcopy of the master thesis